DMD Fast Forward. Published on January 12, 2007 as doi:10.1124/dmd.106.010801

TITLE PAGE:

Role of P-glycoprotein in the Intestinal Absorption of Glabridin, An Active Flavonoid from the Root of *Glycyrrhiza glabra*

Jie Cao, Xiao Chen, Jun Liang, Xue-Qing Yu, An-Long Xu, Eli Chan, Wei Duan, Min Huang, Jing-Yuan Wen, Xi-Yong Yu, Xiao-Tian Li, Fwu-Shan Sheu, Shu-Feng Zhou

Department of General Surgery, the First Municipal Hospital of Guangzhou, Guangzhou, China (J Cao)

Department of Pharmacy, the First Affiliated Hospital, Sun Yat-sen University, Guangzhou, China (X Chen)

Department of Pharmacology and Toxicology, Australian Institute of Chinese Medicine, Sydney, New South Wales 2118, Australia (J Liang & SF Zhou)

Department of Nephrology, the First Affiliated Hospital, Sun Yat-sen University, Guangzhou, China (XQ Yu)

Department of Biochemistry, School of Life Sciences, Sun Yat-sen University, Guangzhou, China (AL Xu)

Department of Pharmacy, Faculty of Science, National University of Singapore, Singapore (E Chan)

School of Pharmacy, Faculty of Medical and Health Sciences, the University of Auckland, Auckland, New Zealand (JY Wen)

Institute of Biotechnology, Deakin University, Waurn Ponds, Victoria 3217, Australia (W Duan)

Institute of Clinical Pharmacology, School of Pharmaceutical Sciences, Sun Yat-sen University, Guangzhou, China (M Huang)

Department of Molecular & Clinical Pharmacology, Guangdong Provincial Cardiovascular Institute. 96 Dongchuan Road, Guangzhou 510080, China (XY Yu)

Department of Maternal Medicine, Obstetrics and Gynecology Hospital, Fudan University, Shanghai, China (XT Li)

Department of Biological Sciences, Faculty of Science, National University of Singapore, Singapore (FS Sheu)

DMD Fast Forward. Published on January 12, 2007 as DOI: 10.1124/dmd.106.010801
This article has not been copyedited and formatted. The final version may differ from this version.

RUNNING TITLE PAGE

a) Running title: PgP and intestinal absorption of glabridin

b) Corresponding author

Dr Shu-Feng Zhou, MD, PhD

Department of Pharmacology and Toxicology, Australian Institute of Traditional Chinese Medicine, 167 Pennant Hills Road, Carlingford, New South Wales 2118, Australia.

Tel: 0061 2 88122471; Fax: 00612 8812 3272

Email: shufengzhou2006@hotmail.com

c) Number of text pages: 52

Number of tables: 4

Number of figures: 13

Number of references: 33

Number of words in *Abstract*: 247

Number of words in *Introduction*: 742

Number of words in *Discussion*: 1483

d) Nonstandard abbreviations: PgP, P-glycoprotein; MDR, multidrug resistance; MRP, multidrug resistance-associated protein; MDCK, Madin-Darby canine kidney; HPLC, high performance liquid chromatography; HBSS, Hank's balanced salt solution; HEPES, *N*-[2-hydroxyethyl] piperazine-N9-[4-butanesulfonic acid]; DMSO, dimethyl sulfoxide; UDPGA, uridine diphosphate glucuronic acid; LC-MS, liquid

DMD Fast Forward. Published on January 12, 2007 as DOI: 10.1124/dmd.106.010801
This article has not been copyedited and formatted. The final version may differ from this version.

chromatography mass spectrometry; MTT, 3-(4,5-dimethylthiazol-2-yl)-2,5-diphenyltetrazonium bromide; i.v., intravenous,; i.p., intraperitoneal; TEER, transepithelial electric resistance; AP, apical; BL, basolateral; $t_{1/2\beta}$, elimination half-life; AUC, the area under the plasma concentration-time curve; C_{max}, maximum plasma concentration; CL, clearance; V_d, volume of distribution; *F*, systemic bioavailability; ANOVA, analysis of variance; P_{lumen}, permeability calculated based on the disappearance of the drug from the intestinal lumen; P_{blood}, permeability calculated based on appearance of the drug in the blood; P_{app}, apparent permeability coefficient; K_m, Michaelis-Menten constant; K_i, inhibition constant.

DMD Fast Forward. Published on January 12, 2007 as DOI: 10.1124/dmd.106.010801
This article has not been copyedited and formatted. The final version may differ from this version.

ABSTRACT:

Glabridin is a major constituent of the root of *Glycyrrhiza glabra*, which is commonly used in treatment of cardiovascular and central nervous system diseases. This study aimed to investigate the role of P-glycoprotein (PgP/MDR1) in the intestinal absorption of glabridin. The systemic bioavailability of glabridin was about 7.5% in rats, but increased when combined with verapamil. In single-pass perfused rat ileum with mesenteric vein cannulation, the permeability coefficient of glabridin based on drug disappearance in luminal perfusates (P_{lumen}) was about 7-fold higher than that based on drug appearance in the blood (P_{blood}). Glabridin was mainly metabolized by glucuronidation and the metabolic capacity of intestine microsomes was 1/15 to 1/20 of that in liver microsomes. Polarized transport of glabridin was found in Caco-2 and MDCKII monolayers. Addition of verapamil in both apical (AP) and basolateral (BL) sides abolished the polarized transport of glabridin across Caco-2 cells. Incubation of verapamil significantly altered the intracellular accumulation and efflux of glabridin in Caco-2 cells. The transport of glabridin in the BL-AP direction was significantly higher in MDCKII cells overexpressing PgP/MDR1 than that in the control cells. Glabridin inhibited PgP-mediated transport of digoxin with an IC_{50} value of 2.56 μM, but stimulated PgP/MDR1 ATPase activity with a K_m of 25.1 μM. The plasma $AUC_{0\text{-}24h}$ of glabridin in *mdr1a*(-/-) mice was 3.8-fold higher than that in wildtype mice. These findings indicate that glabridin is a substrate for PgP and both PgP/MDR1-mediated efflux and first-pass metabolism contribute to the low oral bioavailability of glabridin.

DMD Fast Forward. Published on January 12, 2007 as DOI: 10.1124/dmd.106.010801
This article has not been copyedited and formatted. The final version may differ from this version.

INTRODUCTION:

There is an increasing consumption of herbal medicines in recent years in Asian and Western countries. Their incorporation into medical care system has been encouraged by the World Health Organization despite the lack of evidence for the efficacy of most herbal drugs. Herbal medicines are usually orally administered with long-term regimens. However, the nature of intestinal absorption of the major ingredients of most herbal medicines are unknown, probably due to lack of sensitive analytical methods; difficulties in the choice of the marker components; and difficulties in the establishment and validation of efficient study models. The widely used traditional Chinese medicine, the root of *Glycyrrhiza glabra* (Licorice), is one of the most commonly used herbal medicines in the world due to its exceptional pharmacological properties recognized by traditional Chinese medicine (Zhu, 1998). Licorice has been used as antidotes, demulcents, expectorants, antioxidants, and remedies for inflammation, as well as flavoring and sweetening agents in Asia and Europe (Zhu, 1998). Licorice contains glycyrrhizin, oleane triterpenoids, glucose, and flavonoids. Glabridin (**Figure 1**) is a major polyphenolic flavonoid and a main constituent in the hydrophobic fractions of licorice extract. It has antioxidant, antimicrobial, antiatherosclerotic, hypolipidemic, anti-inflammatory, estrogen-like, hypoglycemic, cardiovascular protective, antinephritic and radical scavenging activities (Belinky et al., 1998; Yokota et al., 1998; Rosenblat et al., 1999; Tamir et al., 2000). The hydroxyl groups on the glabridin B ring were found to be most important for its antioxidative activity (Belinky et al., 1998). Because of the wide spectrum of

DMD Fast Forward. Published on January 12, 2007 as DOI: 10.1124/dmd.106.010801
This article has not been copyedited and formatted. The final version may differ from this version.

pharmacological activity, Licorice is widely used as a single preparation or more often in combination with other herbs to treat diseases in respiratory, cardiovascular, endocrine and digestive system. The Pharmacopoeia of the People's Republic of China recommends dosage of 8–25 g daily for Licorice in decoction form, or up to 100 g in treatment of severe diseases (Zhu, 1998). Since the typical content of glabridin in Licorice is about 0.08–0.35% of dry weight (Hayashi et al., 2003), about 20–87.5 mg of glabridin is administered daily if 25 g crude licorice is dosed (or 80–350 mg when 100 g of crude extract was dosed in some cases). However, in some licorice extract products, the contents of glabridin are up to 1.2–11.6% (Vaya et al., 1997), and 300-2,900 mg of glabridin is taken when 25 g of crude licorice extract is used.

P-glycoprotein (PgP/MDR1) was initially found to be expressed at high levels in many tumor cell lines and conferred multidrug resistance (MDR) to a variety of anticancer drugs, including vinca alkaloids, epipodophyllotoxins, taxanes, and anthracyclines. It is a 170- to 180-kDa plasma membrane protein encoded by the human *MDR1* and *MDR3* genes, the murine *mdr1a*, *mdr1b*, and *mdr2* and rat *pgp1*, *pgp2*, and *pgp3* genes (Borst and Elferink, 2002). However, only the expression of human MDR1, and rodent mdr1a and mdr1b appears to selectively confer MDR. PgP/MDR1 is made up of two symmetrical halves, each of which contains six membrane-spanning domains and an ATP-binding site. Besides its role in conferring MDR, PgP/MDR1 has also been found in many normal tissues, including the

intestinal epithelium, brain capillary endothelial cells, hepatocytes, and renal tubular cells, suggesting its important role in drug absorption, elimination, and distribution (Borst and Elferink, 2002). PgP/MDR1 and other apical ATP-binding cassette transporters such as multidrug resistance associated protein 1 (MRP1) act as a major intestinal barrier, limiting the absorption of a number of lipophilic drugs (Fromm, 2004; Kunta and Sinko, 2004). Oral administration remains the most popular route for most prescribed drugs and herbal medicines due to its convenience and non-invasiveness. However, poor oral absorption is a concern for many drugs and herbal constituents.

Despite the wide use of licorice, the pharmacokinetic properties of glabridin and its interaction with PgP/MDR1 have not been investigated in animals and humans. Data on its absorption, metabolism, distribution and elimination are lacking. This prompted us to investigate the role of PgP/MDR1 in its intestinal absorption using several *in vitro* and *in vivo* models: a) single-pass rat intestinal perfusion with mesenteric vein cannulated; b) Caco-2 cell monolayers; c) monolayers of MDCKII cells over-expressing human PgP/MDR1; d) healthy rats in the presence and absence of combined verapamil; and e) *mdr1a* knockout mice. The single-pass rat intestinal perfusion model allows determination of intestinal absorption of compounds without concern for confounding effects from hepatic first-pass effect. We examined the effects of glabridin on PgP/MDR1-mediated digoxin transport in Caco-2 cells and on PgP/MDR1 ATPase activity. In addition, the metabolism of glabridin in rat intestinal

DMD Fast Forward. Published on January 12, 2007 as DOI: 10.1124/dmd.106.010801
This article has not been copyedited and formatted. The final version may differ from this version.

and hepatic microsomes was investigated.

MATERIALS AND METHODS:

Chemicals and Reagents

Glabridin [(*R*)-4-(3,4-Dihydro-8,8-dimethyl)-2*H*,8*H*-benzo[1,2-*b*:3,4-*b*']dipyran-3yl)-1,3-benzenediol] extracted and purified from the root of *Salvia miltiorrhiza* were purchased from the National Institute for the Control of Pharmaceutical and Biological Products (Beijing, China). This compound has a purity >99.0%, as determined by high performance liquid chromatography (HPLC). Dulbecco's modified Eagle's medium (DMEM), fetal bovine serum, 0.05% trypsin-ethylenediaminetetraacetic acid (EDTA), penicillin-streptomycin, non-essential amino acids, and sterilized Hank's balanced salt solution (HBSS, pH 7.0) containing 25 mM *N*-[2-hydroxyethyl] piperazine-N9-[4-butanesulfonic acid] (HEPES) and 25 mM glucose were obtained from Invitrogen (Sydney, Australia). The Krebs-Ringer buffer (pH 6.8) was used as buffer in rat intestinal perfusion study. Phenol red, trypan blue, propranolol, dimethyl sulfoxide (DMSO), D-saccharic acid 1,4-lactone, verapamil hydrochloride, Brij 58 (polyoxyethylene 20 cetyl ether), nifedipine, probenecid, quinidine sulfate dihydrate, indomethacin, diclofenac, mefenamic acid, mannitol and antipyrine were all purchased from Sigma-Aldrich (St. Louis, MO). α-Nicotinamide adenine dinucleotide phosphate in reduced form (NADPH) and uridine diphosphate glucuronic acid (UDPGA) were purchased from Roche Diagnostics Ltd. (Sydney, Australia). The leukotriene D4 receptor antagonist,

DMD Fast Forward. Published on January 12, 2007 as DOI: 10.1124/dmd.106.010801
This article has not been copyedited and formatted. The final version may differ from this version.

3-[[[3-[2-(7-chloro-2-quinolinyl)-(E)-ethenyl]phenyl][[3-(dimethylamino)-3-oxoprop yl]thio]methyl]thio]propionic acid (MK-571 or L-660,711), was a gift from Dr Ford Hutchinson (Merck Frosst Canada, Inc., Kirkland, Quebec, Canada). Tissue culture plastics and 0.4 μm pore-size 12 mm i.d.. Transwell polycarbonate inserts were from Corning Co. (Acton, MA). The control MDCKII cells with empty vector and its human MDR1-recombinantly transfected derivative, MDR1-MDCKII, were obtained as a kind gift from Professor Piet Borst (The Netherlands Cancer Institute, Amsterdam, The Netherlands). The water used was purified by a Milli-Q purification system (Millipore, Bedford, MA). All other chemicals and reagents were of analytical or HPLC grade as appropriate.

Animals

Male healthy Sprague-Dawley rats (200–260g) were kept in a room under controlled temperature (22 ±1ºC) and automatic day-night rhythm (12 h-cycle) and housed on wire-bottom cages with paper underneath. The ethical approval of this study was obtained from the Ethical Committee of the Australian Institute of Traditional Chinese Medicine, Sydney, Australia. Animals were treated humanely, and the animal experiments were performed in accordance with the Guide for the Care and Use of Laboratory Animals as adopted and promulgated by the National Institutes of Health of the USA (NIH publication No. 85-23, 1985).

DMD Fast Forward. Published on January 12, 2007 as DOI: 10.1124/dmd.106.010801
This article has not been copyedited and formatted. The final version may differ from this version.

Cell Culture

Caco-2 cells were obtained from the American Type Culture Collection (Summit, NJ). Caco-2, control MDCKII and MDR1-MDCKII cells were cultured in DMEM supplemented with 10% fetal bovine serum, 1% nonessential amino acids, and 100 U/ml penicillin and gentamicin in an atmosphere of 5% CO_2 and 90% relative humidity at 37^{o}C. The expression levels of MDR1 in Caco-2 cells, control MDCKII cells, and the MDR1-transfected MDCKII cells were monitored every 2-4 passages by Western blotting analysis.

Cytotoxicity Assay

The cytotoxic effect of glabridin on various cells examined was determined using the 3-(4,5-dimethylthiazol-2-yl)-2,5-diphenyltetrazonium bromide (MTT) assay. Cells were exposed to the drug for 48 h, and the absorbance of formazan, a metabolite of MTT, was measured at a wavelength of 595 nm using a microplate reader (Tecan Instrument Inc., Research Triangle Park, NC). The MTT assays were the means of at least six independent experiments, each performed in replicate of eight for each drug concentration.

Systemic Bioavailability of Glabridin in Rats

The animals were fasted overnight with free access to water prior to drug administration. Glabridin was freshly prepared by dissolving in DMSO and then diluted with distilled water, resulting in a final DMSO concentration of 0.2% (v/v).

DMD Fast Forward. Published on January 12, 2007 as DOI: 10.1124/dmd.106.010801
This article has not been copyedited and formatted. The final version may differ from this version.

Rats were randomized to three groups (n = 6) to receive 5 or 20 mg/kg glabridin by gavage, or 5 mg/kg by intravenous (i.v.) bolus injection through tail vein. Blood samples were collected through jugular vein cannulation into heparinized tubes at pre-determined times over 24 h following drug administration. Plasma was obtained by centrifugation at 5,000*g* for 6 min at 4^{o}C and the plasma was then transferred to clean 1.5-ml tubes. All samples were stored at –20^{o}C until analysis.

Preparation of Rat Intestinal and Hepatic Microsomes

Hepatic and intestinal mucosal tissues were collected from healthy male Sprague Dawley rats (190–250 g) and stored at –80^{o}C. Hepatic and intestinal microsomes were prepared by differential centrifugation as previously described (Zhou et al., 2000). The rat liver homogenates were centrifuged at 9,000*g* for 20 min at 4^{o}C. The supernatant was then centrifuged at 105,000*g* for 1 h at 4^{o}C using an ultracentrifuge with a Type 70 Ti rotor (Beckman Coulter, Inc. Fullerton, CA). Microsomal protein concentration was determined by the bicinchoninic acid method (Smith et al., 1985). Tissue microsomes were stored at –80^{o}C until use.

In vitro Metabolism and Metabolic Inhibition Study in Rat Hepatic and Intestinal Microsomes

Initial incubations containing either 1.0 mg/ml rat hepatic microsomes or 5.0 mg/ml rat intestinal microsomes in the presence of NADPH or UDPGA, were performed to investigate whether Phase I and/or glucuronidation reaction was involved in the

metabolism of glabridin. The depletion of substrate was determined to monitor glabridin metabolism. A single ion monitoring determined the possible formation of new metabolites of glabridin in intestinal and hepatic microsomes using LC-MS. Once any metabolite from Phase I or Phase II reaction was detected, the incubation conditions in hepatic and intestinal microsomes were examined with respect to microsomal protein concentration and incubation time. Typical incubations (200 μl) for glabridin glucuronidation contained hepatic (0.1 mg/ml), or intestinal (1.0 mg/ml) microsomal protein, 10 mM UDPGA, 5 mM $MgCl_2$, 0.1 mg/ml D-saccharic acid 1,4-lactone, Brij 58 (0.1–0.2: 1, ratio of Brij 58 over microsome, w/w), and glabridin (0.1–50 μM) in 0.1 M phosphate buffer (pH 6.8). D-Saccharic acid 1,4-lactone was used to inhibit the activity of β-glucuronidase in microsomes. Typical microsomal incubations (200 μl) for oxidation contained hepatic (1.0 mg/ml) or intestinal (5.0 mg/ml) microsomal protein, 0.5 mM NADPH, 5 mM $MgCl_2$, and glabridin (0.1–50 μM) in 0.1 M phosphate buffer (pH 7.4). All incubations were performed in triplicate, initiated by the addition of UDPGA or NADPH, and conducted at 37^{o}C in a shaking water-bath for 30 min. Incubations were stopped by cooling on ice and adding ice-cold 400 μl acetonitrile: methanol mixture (3: 1, v/v) containing 2 μM IS, and vortexing vigorously. Mixtures were centrifuged at 5,000*g* for 10 min to remove the precipitated microsomal protein. The supernatant was removed and evaporated under nitrogen and the residue reconstituted with 100 μl mobile phase and 20 to 50 μl was injected into the LC-MS for the determination of glabridin and identification of metabolites. The inhibition of hepatic glucuronidation of glabridin in vitro by various

compounds including verapamil, indomethacin, and diclofenac (all at 100 μM) was investigated at various concentrations.

Single Pass Intestinal Perfusion Experiments

The surgical procedures were conducted carefully to prepare the single pass intestinal perfusion with mesenteric vein cannulation as previously described (Zhang et al., 2006). Briefly, rats were anesthetized with 0.5 ml of a cocktail containing ketamine at 75mg/kg and xylazine (Sigma-Aldrich, St Louis, MO) at 5 mg/kg by intraperitoneal (i,p.) injection, and three essential procedures were performed for animals undergoing *in situ* intestinal perfusion: jugular vein cannulation for infusion of blood collected from the donor rats, isolation of an ileum segment for glabridin perfusion, and cannulation of the mesenteric vein for continuous collection of blood samples. Glabridin was infused at 0.1, 0.5, or 2.0 μM with or without the presence of verapamil at 100 μM (a PgP inhibitor), probenecid (200 μM, a MRP1 inhibitor), MK-571 (100 μM, a MRP1/2 inhibitor), or celecoxib (100 μM, a MRP4 inhibitor). The *in situ* intestinal perfusion was initiated by infusing glabridin solution from the syringe pump at 1.0 ml/min for 4 min followed by perfusion at 0.25 ml/min for the remainder of the experiment using a syringe pump ("22" pump, Harvard Apparatus, Holliston, MA). The blood from the mesenteric vein was collected into a heparinized 1.5-ml tube at 5-min intervals over 60 min. In the mean time, perfusate samples were also collected from the outflow of the segment outlet every 5 min into 1.5-ml test tubes over 60 min. The collected blood samples were immediately centrifuged at 5,000*g* for 6 min and

the resultant plasma was transferred to a clean 1.5-ml tube and stored at –20^{o}C until analysis.

The perfusion solution containing 100 μM (≈34.5 μg/ml) phenol red (i.e. phenolsulfonphthalein) was used as a non-absorbable marker for measuring water flux and to correct for changes in the water flux across the incised ileum segment (Zhang et al., 2006). Additional control experiments were conducted to examine the disappearance (in ileum lumen) and appearance (in mesenteric vein blood) rates of the passive transcellular (antipyrine, 100 μM) and paracellular (mannitol, 1.0 mM) markers to validate our single pass rat ileum perfusion system (n = 6 per group). The gut does not metabolize mannitol and antipyrine and absorbs these two compounds in an unchanged form. The effect of verapamil at 100 μM, probenecid at 200 μM, MK-571 at 100 μM, and celecoxib at 100 μM on the intestinal transport of both probe compounds, antipyrine and mannitol, were also investigated.

Uptake and Efflux Study of Glabridin by Cells

The uptake and efflux of glabridin by Caco-2, MDCKII, and MDR1-MDCKII cells were examined in confluent cell cultures grown on 60-mm plastic culture dishes (Corning Co., Acton, MA) as previously described (El Hafny et al., 1997; Zhou et al., 2005). For uptake assay, exponentially growing cells were exposed to 0–50 μM glabridin over 120 min at 37^{o}C. For concentration-dependence study, the incubation time was 30 min. The medium was aspirated off at indicated times, and the dishes

DMD Fast Forward. Published on January 12, 2007 as DOI: 10.1124/dmd.106.010801
This article has not been copyedited and formatted. The final version may differ from this version.

were rapidly rinsed five times with 50 ml of ice-cold phosphate buffered saline (PBS). HPLC analysis ensured that the final wash contained no residual glabridin. The cells were harvested and each cell pellet was suspended in 200 μl extraction solution (acetonitrile: methanol = 1:1, v/v, with 0.01N HCl) with the addition of 10 μl 1.0 mg/ml mefenamic acid which was used as internal standard (IS). For efflux assay, glabridin (0.1–50 μM) was added to confluent cell cultures grown on 60-mm plastic culture dishes (Corning Co., Acton, MA) before three washes with 20 ml warm PBS and incubated for 120 min. After five washes with 4^{o}C PBS of the cells to eliminate the extracellular drug, cells were incubated in culture medium for 20 min at 37^{o}C. After centrifugation of the cells in culture medium at 5,000*g* for 10 min, the supernatant was dried using a rotary concentrator and the residues were reconstituted with the mobile phase and 10–20 μl was then injected into liquid chromatography mass spectrometry (LC-MS) system for glabridin concentration determination. The cellular uptake and efflux of glabridin was expressed as ng/min/mg cellular proteins and corrected by subtraction of the mean extracellular adsorption value of [^{14}C]-sucrose by cells tested.

The effects of various ATP inhibitors (sodium azide at 10 mM and 2, 4-dinitrophenol at 5 mM), PgP and MRP inhibitors, including verapamil, nifedipine (both PgP inhibitors, 100 μM), MK-571 (a MRP1/2 inhibitor, 100 μM), probenecid (a MRP1 inhibitor, 200 μM), and celecoxib (a MRP4 inhibitor, 100 μM), on glabridin cellular uptake and efflux were investigated in Caco-2 cells. All inhibitors were freshly prepared by dissolving in DMSO and then diluted by PBS. The final concentration of

DMD Fast Forward. Published on January 12, 2007 as DOI: 10.1124/dmd.106.010801
This article has not been copyedited and formatted. The final version may differ from this version.

DMSO was 0.2% (v/v). These inhibitors at indicated concentrations showed little cytotoxicity (<8.0%) to the cells tested using MTT assay when incubated for 2 h. All inhibitors were pre-incubated with cells for 2 h. Thereafter, cells were washed with cold PBS buffer five times. The cells were then harvested, lysed by sonication and extracted using ice-cold acetonitrile: methanol mixture (1:1, v/v, with 0.01N HCl) as described above. All uptake and efflux assays in the absence and presence of inhibitor were studied in at least three independent experiments. DMSO at a final concentration of 0.2% (v/v) in the culture buffer, used to dissolve the all inhibitors, did not change the accumulation of glabridin in Caco-2 and MDCKII cells.

The uptake of a known PgP substrate, daunomycin was performed with or without 100 μM verapamil as described above. Preliminary experiments showed that daunomycin uptake was at equilibrium after 60–90 min of incubation in Caco-2 cells. Cells were thus incubated for 30 min with 1.0 μM daunomycin (0.3 μCi/well [^{3}H]-daunomycin (Perkin Elmer, Boston, MA) and unlabelled daunomycin with or without 100 μM verapamil. Cells were then washed with HBSS and it was further processed as described above. In addition, control uptake assays were performed using the extracellular marker [^{14}C]-sucrose (565 mCi/mmol) and [^{3}H]-propranolol (both from Amersham, Buckinghamshire, UK). For efflux assay, [^{3}H]-vinblastine (Amersham, Buckinghamshire, UK) was used as a model substrate, and the radioactivity was determined by LC-6000 liquid scintillation counter (Beckman Instruments, Fullerton, CA).

DMD Fast Forward. Published on January 12, 2007 as DOI: 10.1124/dmd.106.010801
This article has not been copyedited and formatted. The final version may differ from this version.

Transport Study of Glabridin in Caco-2, Control MDCKII and MDR1-MDCKII Monolayers

For the transport studies of glabridin, Caco-2 cells, control MDCKII or MDR1-MDCKII cells were seeded at a density of 5–10 $\times$ 10^5 cells/well onto polycarbonate membrane Transwell inserts (Corning Co., Acton, MA) in 12-well plates. The effective transepithelial electric resistance (TEER) of the monolayers (= total TEER value – value in empty filter membranes) was examined routinely before and after the experiment using a Millicell-ERS apparatus (Millipore Co., Billerica, MA). Caco-2 cells were used for transport experiments 21 days after cell seeding when the effective TEER values typically exceeded 260–350 $\Omega \bullet cm^2$. The transport experiments in Caco-2 cells were conducted on cells between passages 30–35. For MDCKII and MDR1-MDCKII cells, only cells at passages 5–9 were used for transport studies after receipt from the Netherlands Cancer Institute. Cells were used in transport experiments at days 5 to 7 after cell seeding where the effective TEER values for MDCKII monolayers were typically 40–60 $\Omega \bullet cm^2$ and 120–150 $\Omega \bullet cm^2$ for MDR1-MDCKII monolayers. ^{14}C-Mannitol (Amersham, Buckinghamshire, UK) was used as a probe for paracellular transport and a value of 0.5% per hour indicated acceptable integrality for the monolayers examined. The transport of glabridin by Caco-2, control MDCKII, and MDR1-MDCKII monolayers was investigated on an orbital shaker as previously described (Zhang et al., 2006). Briefly, the monolayers were washed twice with warm HBSS containing 25 mM HEPES (pH 7.0) prior to the

DMD Fast Forward. Published on January 12, 2007 as DOI: 10.1124/dmd.106.010801
This article has not been copyedited and formatted. The final version may differ from this version.

transport experiments. A pH of 7.0 was chosen as it was close to the ileum pH value and this pH resulted in maximum apical (AP) to basolateral (BL) and BL to AP transport of glabridin. Nine independent incubations were performed in triplicate for all experiments.

The effects of pH, Na^+, temperature and ATP on glabridin transport across Caco-2 monolayers were investigated. The effect of apical or basolateral pH (5.5–7.4) on the AP to BL and BL to AP flux of glabridin at 0.1 and 1.0 μM was examined at pH 7.4 for the receiving side. The pH was altered by substituting appropriate amounts of HEPES in the incubation medium by equimolar (25 mM) 2-[*N*-morpholino]ethanesulfonic acid. In experiments to investigate the effect of Na^+ on the flux of glabridin at 0.1 and 1.0 μM across the Caco-2 monolayers, sodium chloride in the HBSS was replaced by equimolar amounts (140 mM) of potassium chloride. In addition, the permeability of glabridin from AP to BL and BL to AP was measured after incubation for 30 min at 4°C or 37°C. To determine whether there was a energy dependency of glabridin flux in Caco-2 cells, the transport medium depleted in glucose was used in both sides of the monolayers. Like all other ABC transporters, PgP acts as an efflux pump by exporting its substrate from the membrane or cell cytosol to the exterior of the cells, with ATP hydrolysis as the driving force. Sodium azide (10 mM), or 2, 4-dinitrophenol (5.0 mM) (both ATPase inhibitors), was added to both AP and BL side and the monolayers were incubated for 30 min at 37°C. In experiments to investigate the effects of verapamil (100 μM), probenecid (200 μM),

MK-571 (100 μM), and celecoxib (100 μM) on the transport of glabridin (0.1 and 1.0 μM) from AP to BL and BL to AP directions in the Caco-2 monolayers, the inhibitor was added to the incubation medium on both AP and BL sides of the monolayers throughout the experiment and also pre-incubated with the cells for 2 h before addition of glabridin. All inhibitors were freshly prepared using DMSO prior to the experiment, with a final DMSO concentration of 0.2% (v/v). Vehicle (0.2% DMSO) was used for the control inserts. All collected transport buffer samples containing glabridin were stored at −20°C until analysis using a validated LC-MS method. All incubations were performed in triplicate to nine times. To avoid inter-day cell-cell variations, the transport experiments for the determination of transport kinetics or inhibition by various compounds were conducted on the same day using the same batch of cellular monolayers.

Inhibition of Digoxin Transport by Glabridin in Vitro

Caco-2 cells were grown and cultured on 0.4-μm polycarbonate membrane Transwell inserts (Corning Co., Acton, MA). Transport of [^{3}H]-digoxin (Amersham, Buckinghamshire, UK) at 5.0 μM (15 Ci/mmol) was determined by its addition to the BL side of the Caco-2 monolayer and by measuring the transport of radioactivity into the receiving compartment over 1 h, in the absence or presence of glabridin (0.1–100 μM), or the positive control, verapamil (0.25–100 μM), added in both sides.

DMD Fast Forward. Published on January 12, 2007 as DOI: 10.1124/dmd.106.010801
This article has not been copyedited and formatted. The final version may differ from this version.

P-Glycoprotein ATPase Activity Assay

The effect of glabridin on PgP/MDR1 ATPase activity was determined using ABC Transporter ATPase assay reagent kit consisting of human PgP/MDR1 membrane and PgP/MDR1-negative control membrane fractions, buffers, solutions and relevant reagents (Nacalai Tesque Inc., Kyoto, Japan). Briefly, human PgP/MDR1 membrane or PgP/MDR1-negative control membrane (20 μg) was pre-incubated at 37°C for 5 min in 50 μl of reaction buffer and glabridin (0.1–100 μM) in the presence or absence of 50 μM sodium orthovanadate in a 96-well microplate (Invitrogen, Sydney, Australia). The ATPase reaction was initiated by the addition of 25 μl of 10 mM MgATP solution. The reaction was stopped after 30 min by addition of 30 μl of 10% (w/v) sodium dodecyl sulfate solution, and the amount of phosphate was determined immediately by adding 200 μl of detection solution (1:4, 35 mM ammonium molybdate in 15 mM zinc acetate, pH 5.0, and 10% ascorbic acid, pH 5.0) and incubated at 37°C for 20 min in the dark. The amount of inorganic phosphate complex was determined by measuring the absorbance at 750 nm wavelength by comparing the absorbance to a blank phosphate buffer (pH 7.4) as a standard using a microplate spectrometer (Tecan Instrument Inc., Research Triangle Park, NC). The vanadate-sensitive ATP hydrolysis was determined by subtracting the value obtained with the vanadate co-incubated membrane fractions from vanadate-free membrane fractions. Verapamil (0.25–100 μM) was used as the positive control in these experiments. To estimate the reaction kinetics by glabridin and verapamil, ATP hydrolysis rate was fitted to several non-linear kinetic models using the Prism 3.0

program (Graphpad Software Inc., San Diego, CA).

Effects of Coadministered Verapamil on the Plasma Pharmacokinetics of Glabridin in Rats

In separate kinetic experiments, we examined the effects of coadministered verapamil at 25 or 100 mg/kg on the plasma pharmacokinetics of glabridin in healthy male Sprague Dawley rats. The dose of verapamil selected was approximately the maximum tolerated dose, as assessed in pilot experiments in male Sprague Dawley rats. Rats were randomized to receive the following different treatment (n = 6 per group): glabridin at 5 mg/kg by gavage plus water (0.3 ml, control vehicle); and glabridin at 5 mg/kg by gavage in combination with verapamil at 50 or 100 mg/kg by oral gavage dissolved in water; The inhibitor was administered 2 h before glabridin dosing. Blood was collected as described above. The concentrations of glabridin in plasma were determined by LC-MS.

Pharmacokinetic Study of Glabridin in *mdr1a*(-/-) Gene-deficient and Wildtype Mice

FVB/NJ (20–35 g) and *mdr1a* gene-deficient mice (25–30 g) were purchased from Jackson Laboratories (Bar Harbor, ME) and Taconic Farms, Inc. (Germantown, NY), respectively. The mice were treated with oral glabridin at 5 mg/kg by gavage (n = 4 per time points). At pre-determined time points, the mice were sacrificed by neck dislocation. Blood were immediately collected and plasma was obtained by

DMD Fast Forward. Published on January 12, 2007 as DOI: 10.1124/dmd.106.010801
This article has not been copyedited and formatted. The final version may differ from this version.

centrifugation at 5,000*g* for 10 min at 4°C and all tissues were process as described above. The concentration of glabridin in plasma and tissues was determined by LC-MS analysis.

Liquid Chromatography Mass Spectrometry and High Performance Liquid Chromatography Analysis of Glabridin

The concentrations of glabridin in rat and mouse plasma, perfusates, transport medium in cellular monolayers and cellular lysates were determined by an LC-MS system equipped with an Agilent 1100 LC connected to an Applied Biosystems Q-Trap 4000 mass spectrometer through an electrospray ionization source. Chromatographic separation was achieved using a C18 Hyperclon ODS column (200 mm × 4.6 mm i.d.) (Phenomenex, Torrance, CA) preceded by a Phenomenex C18 guard cartridge at room temperature (22°C). Mobile phase composed of methanol and 0.1% (v/v) formic acid (85:15, v/v) had a flow rate of 0.2 ml/min. Injection volume was 20 μl of a sample kept in an autosampler set at 10°C. Air set at 600°C and a pressure of 70 psi was used for heating, and the nebulizing gas was set at 40 psi. The capillary temperature was 450°C and the spray voltage was 4,000 V. The product ions were recorded using a negative ion detection mode. The monitored ions and collision energy were *m*/*z* 323.1 → 201.3 and 30 eV for glabridin, and *m*/*z* 240.1 → 196.1 and 25 eV for the IS. The lower limit of quantitation of glabridin was 0.025–0.05 ng/ml in rat and mouse plasma, perfusates and other matrices tested in this study. Glabridin was recovered by >95%, and was stable when kept at 10°C for 36 h, at −20 °C for 3

months, and after five-eight freeze-thaw cycles.

The antipyrine and mannitol in perfusates were determined by a validated HPLC method as described previously (Miki et al., 1996; Hung et al., 2001). The lower limit of quantitation for antipyrine and mannitol was 30.0 and 195.0 ng/ml, respectively.

Pharmacokinetic Calculation

The plasma concentration-time curves of glabridin in rats were obtained by plotting the mean plasma concentrations of glabridin versus time on a semi-logarithmic scale. Pharmacokinetics parameters were calculated by standard model-independent pharmacokinetic formulae using WinNonlin program (Pharsight Inc., Mountain View, CA). The elimination half-life ($t_{½\beta}$) value was calculated as 0.693/β, where β is the elimination rate constant calculated from the terminal linear portion of the log plasma concentration-time curve. The total areas under plasma concentration-time curve from time zero to the last quantifiable time point (AUC_{0-t}) and from time zero to infinity ($AUC_{0-\infty}$) were calculated using the log trapezoidal rule. The $AUC_{0\rightarrow\infty}$ was calculated as following equation:

$$AUC_{0\rightarrow\infty} = AUC_{0-t} + C_t/\beta \qquad (1)$$

where C_t is the last measurable plasma concentration. The maximum plasma concentration (C_{max}) for glabridin was obtained by visual inspection of the plasma concentration-time curve, whereas the initial drug concentration (the extrapolated concentration at zero time) of the drug following i.v injection was calculated by back

DMD Fast Forward. Published on January 12, 2007 as DOI: 10.1124/dmd.106.010801
This article has not been copyedited and formatted. The final version may differ from this version.

extrapolation of the plasma concentration-time curve to Y-axis. The plasma clearance (CL) was estimated by dividing the total administered dose by the $AUC_{0-\infty}$. The volume of distribution (V_d) was calculated by dividing CL by β.

The systemic bioavailability (*F*, %) of glabridin after oral administration was determined as follow:

$$F\,(\%) = (AUC^{p.o.}/Dose^{p.o.})/(AUC^{i.v.}/Dose^{i.v.}) \times 100 \qquad (2)$$

Where $AUC^{p.o.}$ and $AUC^{i.v.}$ were the areas under the plasma concentration curves calculated after oral and i.v. administration, respectively.

Data Analysis

Data are presented as mean ± S.D. The initial statistical analysis to evaluate the differences in the mean kinetic parameters among the different groups was carried out by a one-way analysis of variance (ANOVA) followed with a post-hoc test (Dunnett's multiple comparison test). The Student's *t*-test was conducted for the between-group comparisons with a significance level of $P < 0.05$.

The permeability values of glabridin across rat ileum were calculated based on the disappearance of the drug from the lumen (P_{lumen}) as well as the appearance of drug in the blood (P_{blood}) using the following equations (Zhang et al., 2006):

$$P_{lumen} = -\frac{Q}{2\pi rl}\ln\frac{C_{lumen}}{C_0} \qquad (3)$$

DMD Fast Forward. Published on January 12, 2007 as DOI: 10.1124/dmd.106.010801
This article has not been copyedited and formatted. The final version may differ from this version.

$$P_{\text{blood}} = \frac{dX/dt}{A \times C_0} \quad (4)$$

where r was the radius of the intestinal lumen (0.18 cm), l was the length of the segment (cm), Q was the flow rate of drug through the intestinal segment, C_0 was the concentration of glabridin at the start of perfusion (in the syringe), C_{lumen} was the steady-state concentration of glabridin exiting the lumen, dX/dt was the rate of glabridin appearance in mesenteric venous blood (μg/sec), and A was the surface area of the ileum segment (= $2\pi rl$, cm^2).

The apparent permeability coefficient (P_{app}) in cellular monolayers is expressed in cm/sec, and calculated as following equation

$$P_{app} = \frac{\Delta Q}{\Delta t} \times \frac{1}{60} \times \frac{1}{A} \times \frac{1}{C_0} \quad (5)$$

where $\Delta Q/\Delta t$ is the permeability rate (μg/sec); A is the surface area of the membrane (cm^2); and C_0 is the initial drug concentration in the donor chamber (μg/ml). Samples from 30 min point were used for P_{app} calculations as at this time steady state has achieved. The net BL to AP efflux of glabridin (R_{net}) was determined by calculating the ratio of P_{app} in the BL to AP direction vs P_{app} in the AP to BL direction ($P_{app(BL-AP)}/P_{app(AP-BL)}$) as Eq. 6 (Zhou et al., 2005).

$$R_{net} = \frac{P_{app(BL-AP)}}{P_{app(AP-BL)}} \quad (6)$$

The passive diffusion flux rate (excluding the influence of efflux transporter) of glabridin in Caco-2 monolayers was estimated by conducting the transport experiment in the presence of verapamil (100 μM) assuming that other transporters play a

DMD Fast Forward. Published on January 12, 2007 as DOI: 10.1124/dmd.106.010801
This article has not been copyedited and formatted. The final version may differ from this version.

minimal role in glabridin transport. The active transport flux rates were then estimated by subtracting the passive diffusion rates from total flux rates. Several models to describe the kinetics of the calculated active transport and ATPase stimulation activity of glabridin (single and two binding sites with and without a non-saturable component, substrate inhibition, and the sigmoid models) were fitted with the following models and using the Prism 3.0 program (Graphpad Software Inc., San Diego, CA).

$$v = \frac{V_{max}[S]}{K_m + [S]} \quad (7)$$

$$v = \frac{V_{max}[S]}{K_m + [S]} + K_d \quad (8)$$

$$v = \frac{V_{max1} \times [S]}{K_{m1} + [S]} + \frac{V_{max2} \times [S]}{K_{m2} + [S]} \quad (9)$$

$$v = \frac{V_{max1} \times [S]}{K_{m1} + [S]} + \frac{V_{max2} \times [S]}{K_{m2} + [S]} + K_d \quad (10)$$

$$v = \frac{V_{max} \times [S]}{K + [S] + [S]^2 / K_{is}} \quad (11)$$

$$v = \frac{V_{max} \times [S]^{h'}}{K^{h'} + [S]^{h'}} \quad (12)$$

where v is the rate of glabridin transport or ATP hydrolysis; V_{max}, is the maximum velocity; K_m, Michaelis-Menten constant; [S], the substrate concentration; K_d, the non-saturable component; K_{is}, the substrate inhibition constant; h', the Hill coefficient for cooperative substrate binding; and subscripts 1 and 2 represent the first and the second type of enzyme binding sites. The choice of model was confirmed by *F*-test and comparison of Akaike's information criterion values (Yamaoka et al., 1978).

DMD Fast Forward. Published on January 12, 2007 as DOI: 10.1124/dmd.106.010801
This article has not been copyedited and formatted. The final version may differ from this version.

Apparent inhibition constant (K_i) was estimated using Eq. 13-15 as previously described (Zhou et al., 2005).

$$K_i = \frac{P_I / P_0}{1 - (P_I / P_0)}[I] \quad (13)$$

$$P_0 = P_{app_1} - P_{app_3} \quad (14)$$

$$P_I = P_{app_2} - P_{app_3} \quad (15)$$

where P_I and P_0 are the P_{app} values of glabridin in the direction of BL to AP in the presence and absence of the inhibitor, respectively; and P_I/P_0 is a reflection of the inhibitory effect of the test compound on the active BL to AP transport of glabridin across the Caco-2 monolayers. [*I*] is the concentration of inhibitor in the donor and the receiver side. P_{app1} is the total transport in the absence of any inhibitory compound; P_{app2} is the total transport in the presence of a potential inhibitor; and P_{app3} is the passive diffusion component.

DMD Fast Forward. Published on January 12, 2007 as DOI: 10.1124/dmd.106.010801
This article has not been copyedited and formatted. The final version may differ from this version.

RESULTS:

Oral Bioavailability of Glabridin in Rats

The representative plasma concentration-time profiles of glabridin after oral (5 and 20 mg/kg), and i.v. (5 mg/kg) administration in rats are shown in **Figure 2** and the pharmacokinetic parameters of glabridin are listed in TABLE 1. After oral administration of glabridin at 5 or 20 mg, the C_{max}, T_{max} and $AUC_{0\text{-}24h}$ of glabridin was 15.10 ± 4.72 ng/ml and 60.41 ± 18.87 ng/ml; 4.33 ± 1.86 h and 4.50 ± 2.17 h; and 96.49 ± 32.34 ng/ml•h and 387.98 ± 137.28 ng/ml•h, respectively. These results showed that the oral pharmacokinetics of glabridin is linear (dose-independent), as indicated by the proportional increase of C_{max} and AUC of glabridin when its oral dose was increased from 5 mg/kg to 20 mg/kg. The $t_{1/2\beta}$ of glabridin was 2.38–2.41 h after administration at 5–20 mg/kg.

In addition, following i.v. bolus injection of glabridin at 5 mg/kg, the C_{max}, $AUC_{0\text{-}24h}$, $t_{1/2\beta}$, CL and V_d were 1.92 h, 1301.48 ± 375.79 ng/ml•h, 1.92 h, 59.01 ml/min/kg and 2.72 L/kg, respectively. Thus, the *F* values of glabridin in rats were 7.45% and 7.44%, respectively, following oral dosing of glabridin at 5 and 20 mg/kg. These findings indicate that the oral absorption and oral bioavailability of glabridin is low and dose-independent.

In vitro Metabolism of Glabridin in Rat Intestinal and Hepatic Microsomes

In rat intestinal and hepatic microsomes, no oxidative metabolites of glabridin were

observed when glabridin was incubated in the presence of NADPH using LC-MS and HPLC methods. Marked formation of glabridin glucuronide was found when glabridin was incubated with rat hepatic microsomes in the presence of UDPGA. The formation of glabridin glucuronide, when monitored by relative metabolite ion density using LC-MS, was linear up to 60 min incubation time and 50 μM substrate concentration. A minimal peak of glabridin glucuronide using HPLC and a weak signal of glabridin glucuronide ion using LC-MS was observed when the substrate was incubated in rat intestinal microsomes. The formation rate of glabridin glucuronide in rat intestinal microsomes was about 1/15–1/20 of that when incubated with rat hepatic microsomes. In addition, diclofenac and indomethacin (both at 100 μM) inhibited the formation of glabridin glucuronide in rat hepatic and intestinal microsomes by 68.5 ± 15.2% and 72.3 ± 14.3%, respectively. However, verapamil at 100 μM did not inhibit glabridin glucuronidation in both intestinal and hepatic microsomes.

Transport of Glabridin in Single-Pass Perfusion Study of Rat Ileum

There was insignificant loss of glabridin (<6.0%) when the drug was perfused through the perfusion apparatus used in this study, indicating that there was no significant adsorption of glabridin to the tubing wall of the system. The compound was stable in the perfusion buffer as well as intestinal perfusate at 37^{o}C for at least 12 h.

There were no oxidative metabolites formed in the perfusates or mesenteric vein

DMD Fast Forward. Published on January 12, 2007 as DOI: 10.1124/dmd.106.010801
This article has not been copyedited and formatted. The final version may differ from this version.

blood after glabridin was loaded as determined by both HPLC and LC-MS analysis. No detectable peak of glabridin glucuronide in the perfusates or mesenteric vein blood was found using HPLC analysis, but a weak signal of glabridin glucuronide ion using LC-MS was observed. This indicated that the glucuronidation of glabridin by rat perfused ileum segment was minimal or just detectable, and gut metabolism had a minor impact to the determination of permeability coefficients of glabridin in this model.

For intestinal perfusions with glabridin, samples were collected from the outlet of the ileum segment and mesenteric vein at 5-min intervals over 60 min. The permeability values of glabridin at 0.1, 0.5 and 2.0 μM are shown in TABLE 2. The permeability of glabridin based on the luminal disappearance of the compound was estimated at steady state (i.e. samples obtained from 30–60 min). The P_{lumen} values of glabridin were 6.51 $\pm$ 0.72 $\times$ 10^{-4}, 8.22 $\pm$ 0.91 $\times$ 10^{-4}, and 11.54 $\pm$ 1.31 $\times$ 10^{-4} cm/sec, respectively, when the concentration of glabridin in perfusates were 0.1, 0.5 and 2.0 μM. With the increase of glabridin concentration in perfusates, the P_{lumen} values significantly increased ($P < 0.05$). The appearance of glabridin in mesenteric vein blood increased when the drug concentration was 0.1, 0.5 and 2.0 μM in perfusates. The concentration-dependent increase in P_{lumen} of glabridin may reflect the relatively low to moderate intrinsic permeability of glabridin and possible involvement of saturable active mechanism for its intestinal transport. As for the permeability based on appearance of glabridin in the mesenteric blood (P_{blood}), concentration-dependent

DMD Fast Forward. Published on January 12, 2007 as DOI: 10.1124/dmd.106.010801
This article has not been copyedited and formatted. The final version may differ from this version.

increase in permeability were evident, whereas the P_{blood} values at 0.1, 0.5 and 2.0 μM was 6.5- to 7.0-fold lower than P_{lumen} ($P < 0.05$).

Verapamil, probenecid, MK-571 and celecoxib all did not significantly alter the P_{lumen} values of glabridin at 0.1, 0.5, or 2.0 μM ($P > 0.05$). However, the P_{blood} values of glabridin at 0.1, 05, and 2.0 μM increased significantly in the presence of 100 μM verapamil, with the ratio of P_{lumen}:P_{blood} decreased from 7.5–8.0 to 3.0–3.3 (TABLE 2). However, probenecid, MK-571 and celecoxib insignificantly affected the P_{blood} values at all substrate concentrations tested. These data suggest that PgP-mediated efflux effectively limited the absorption of glabridin across the intestinal wall, which was at least partially reversed by verapamil, a known PgP inhibitor, but not by MRP inhibitors including probenecid (MRP1), MK-571 (MRP1/2) and celecoxib (MRP4).

We also examined the transport of two probe compounds, antipyrine (a well-absorbed passive transcellular transport marker) and mannitol (a well-absorbed paracellular transport marker), using the single pass intestinal perfusion model. The results showed that the P_{lumen} and P_{blood} for antipyrine were $5.96 \pm 1.33 \times 10^{-5}$ cm/sec and $6.12 \pm 2.21 \times 10^{-5}$ cm/sec (n = 6 per group), respectively; and $7.63 \pm 1.25 \times 10^{-6}$ and $7.74 \pm 1.68 \times 10^{-6}$ cm/sec for mannitol, respectively. The addition of verapamil at 100 μM or other inhibitor did not significantly affect the P_{lumen} and P_{blood} of both antipyrine and mannitol (data not shown). Notably, the P_{lumen} values of glabridin were significantly higher than those for antipyrine and mannitol. These results indicate that

DMD Fast Forward. Published on January 12, 2007 as DOI: 10.1124/dmd.106.010801
This article has not been copyedited and formatted. The final version may differ from this version.

there was no significant difference between P_{lumen} and P_{blood} for antipyrine and mannitol and our single pass intestinal perfusion model was a valid system for study of drug transport.

Cytotoxicity and Metabolism of Glabridin in Caco-2, control MDCKII, and MDR1-MDCKII Cells

Glabridin at 0.1−100 μM did not show significant cytotoxicity (<10%) to Caco-2, control MDCKII, and MDR1-MDCKII cells when incubated for up to 48 h as determined by the MTT assay.

No detectable oxidative metabolites were observed when glabridin at 0.1−100 μM was incubated with Caco-2, control MDCKII and MDR1-MDCKII cells for 2−48 h as determined by HPLC and LC-MS analysis. A minor signal was detected for glabridin glucuronide ion when the substrate was incubated with Caco-2 for 2-48 h, as determined by LC-MS analysis. The minimal formation of glabridin glucuronides in Caco-2 cells indicated that Caco-2 cells had a weak metabolic ability to glabridin possibly due to low levels or activity of uridine diphosphate glucuronosyltransferases that metabolize this compound and metabolism had a minor impact to the assessment of transport of glabridin in this model.

Uptake and Efflux of Glabridin in Caco-2 Cells

The intracellular accumulation and efflux of glabridin in Caco-2 cells was examined

DMD Fast Forward. Published on January 12, 2007 as DOI: 10.1124/dmd.106.010801
This article has not been copyedited and formatted. The final version may differ from this version.

with regard to incubation time and substrate concentration (**Figure 3**). The uptake of glabridin into Caco-2 cells was linear up to 60 min, whereas efflux of glabridin out of Caco-2 cells was linear up to 20 min. Its accumulation and efflux in Caco-2 cells also increased depending on the substrate concentration and followed Michaelis-Menten kinetics with one-binding site model being the best fit. The estimated K_m and V_{max} for glabridin uptake by Caco-2 cells and efflux from Caco-2 cells were 12.38 ± 1.41 and 4.68 ± 1.03 μM; and 17.44 ± 0.76 ng/min/mg cellular protein and 0.67 ± 0.04 pg/min/mg cellular protein, respectively. We also monitored the intracellular concentration of glabridin at 1.0 μM upon incubation over 120 min (**Figure 3**). It appeared that the efflux of glabridin from Caco-2 cells was characterized by a mono-exponential kinetics with a half life of 9.84 min, indicating a rapid exit of the drug from Caco-2 cells during the first 10 min, followed by a slow exit requiring several hours.

The effects of 2-h pre-incubation of potential inhibitors including verapamil, nifedipine, probenecid, MK-571, and celecoxib on the intracellular accumulation and efflux of glabridin in Caco-2 cells are shown in **Figure 4**. When verapamil or nifedipine (both at 100 μM) was pre-incubated for 2 h with the cells, glabridin accumulation was significantly ($P < 0.05$) increased by 83.3 ± 13.3% and 116.9 ± 15.2 %, respectively. Addition of MK-571 (100 μM), celecoxib (100 μM), or probenecid (200 μM), insignificantly increased glabridin intracellular accumulation by 2.4−13.5% ($P > 0.05$). On the other hand, when verapamil or nifedipine (both at 100 μM) was

DMD Fast Forward. Published on January 12, 2007 as DOI: 10.1124/dmd.106.010801
This article has not been copyedited and formatted. The final version may differ from this version.

pre-incubated in Caco-2 cells for 2 h, glabridin efflux was significantly ($P < 0.05$) decreased by 27.8 ± 3.3% and 32.5 ± 4.2 %, respectively. Addition of MK-571 (100 μM), celecoxib (100 μM), or probenecid (200 μM), insignificantly increased glabridin efflux ($P > 0.05$). These findings demonstrated that pre-incubation for 2 h with the PgP inhibitors, verapamil and nifedipine, instead of MRP inhibitors including MK-571, probenecid and celecoxib, significantly altered glabridin accumulation in Caco-2 cells and efflux from Caco-2 cells, suggesting that glabridin is likely a substrate for PgP/MDR1, but not for MRP1-4. A significantly altered glabridin accumulation in Caco-2 cells and efflux from these cells by addition of verapamil or nifedipine, but not MK-571, probenecid and celecoxib, suggested that glabridin is likely a substrate for PgP/MDR1, but not for MRP1-4.

Uptake of the probe markers, sucrose and propranolol, into Caco-2 cells was determined upon incubation up to 120 min. Propranolol penetrated into Caco-2 cells to a low extent (0.25 ± 0.03 – 0.44 ± 0.52 ng/min/mg cellular protein), and diffusion of sucrose into the cells was minimal (0.04 ± 0.00 – 0.07 ± 0.01 ng/min/mg cellular protein). The uptake of sucrose and propranolol did not increase with incubation time and substrate concentration in Caco-2 cells. In addition, daunomycin as a model PgP/MDR1 substrate, its uptake by Caco-2 cells was significantly increased by 75.2 ± 9.4% when co-incubated with 100 μM verapamil. In addition, the efflux of the model substrate vinblastine was also dependent on the substrate concentration and incubation time, but its cellular efflux was characterized by a biexponential kinetics with half-lives

9.8 min and 2.7 h, respectively.

Transport of Glabridin in Caco-2 Monolayers

After incubation of glabridin at 0.1–50 μM loaded at either AP or BL side, the sample was collected from the receiving side for LC-MS analysis. No detectable metabolites were observed when glabridin was loaded on AP or BL side at all concentrations over 60 min. The time course and concentration effect of glabridin flux from AP to BL or BL to AP have been examined and the results are shown in **Figure 5**. After AP or BL drug loading, glabridin appeared on the receiving side by 5 min. The flux rate (ng/min/cm^2) of glabridin from AP to BL or BL to AP side was largely proportional to glabridin concentrations over 0.1–50 μM and was linear up to 60 min of incubation time. The transport rate of glabridin across Caco-2 monolayers from BL to AP side was significantly ($P < 0.05$) higher than that from AP to BL side. The P_{app} of glabridin from BL to AP side (8.12–25.63 $\times$ 10^{-5} cm/sec) was about 3.3- to 8.4-fold higher than those from AP to BL side (0.87–5.76 $\times$ 10^{-5} cm/sec) with a marked decrease in P_{app} values for both directional transport at increasing glabridin concentration (**Figure 5**). The R_{net} values ranged from 4.3 to 9.4. These results demonstrated a polarization in the Caco-2 permeability toward glabridin and a predominantly secretory rather than absorptive transport. The BL to AP efflux rate of glabridin increased with increasing glabridin concentrations over 0.1–50 μM but appeared saturable when glabridin concentration was ≥10 μM as indicated by a non-proportional increase in the efflux (data not shown). Consistently, there was a

DMD Fast Forward. Published on January 12, 2007 as DOI: 10.1124/dmd.106.010801
This article has not been copyedited and formatted. The final version may differ from this version.

significant decrease in P_{app} values for BL to AP flux at glabridin concentrations ≥10 μM ($P < 0.001$).

The passive and active AP-BL and BL-AP transport was calculated only based on verapamil inhibition of PgP in Caco-2 cells assuming that the role of other transporters for glabridin transport is minimal and negligible. Model fitting indicates that one binding-site model was the best fit for calculated active BL to AP efflux, with a K_m of 6.57 ± 1.16 μM, and V_{max} of 0.65 ± 0.03 nmol/min/cm^2 as shown in **Figure 6**. The low K_m value suggested that glabridin was a substrate for PgP with high affinity.

Reducing the apical pH to 5.5–6.5 caused a significant ($P < 0.05$) increase glabridin flux by 24.5–56.8% at 0.1 and 1.0 μM from AP to BL or BL to AP side compared to the values at pH 7.4. A maximum P_{app} was observed at pH 7.0 for both AP-BL and BL-AP transport at 0.1 and 1.0 substrate concentration. Lower pH may reduce the ionization of glabridin and thus increase its intestinal transport. The substitution of sodium salts in the transport medium with potassium salts had no significant effect on the flux of glabridin for either AP to BL or BL to AP direction, suggesting that the active transporter system for glabridin was sodium-independent. Reducing the incubation temperature from 37^{o}C to 4^{o}C significantly ($P < 0.05$) decreased the flux of glabridin at 0.1 and 1.0 μM from AP to BL or BL to AP side, with a 42.2–75.5% reduction of the P_{app} values (data not shown). Moreover, the absence of glucose in the transport medium did not significantly affect the AP to BL flux of glabridin at either

DMD Fast Forward. Published on January 12, 2007 as DOI: 10.1124/dmd.106.010801
This article has not been copyedited and formatted. The final version may differ from this version.

0.1 or 1.0 μM. In contrast, depletion of glucose significantly ($P < 0.05$) decreased the BL to AP flux of glabridin at 0.1 and 1.0 μM by 50.5–65.2%. These results indicated that the transport of glabridin across Caco-2 monolayers was pH-, energy-, and temperature-dependent, but not sodium-dependent.

The effects of ATP inhibitors and various ABC transporter inhibitors on the transport of glabridin (0.1 and 1.0 μM) in Caco-2 monolayers were also investigated. Addition of the transport buffer at both sides with sodium azide (10 mM), 2, 4-dinitrophenol (1 mM), or verapamil (100 μM), significantly ($P < 0.05$) increased the AB to BL flux of glabridin at 0.1 μM by 52.8%, 38.6%, and 82.4%, respectively ($P < 0.05$) (**Figure 7**). In contrast, these compounds caused a significant ($P < 0.05$) decrease in the BL to AP flux of glabridin at 0.1 μM by 48.4%, 43.3%, and 53.1%, respectively. Similar results were observed when the concentration of glabridin was increased to 1.0 μM in the presence of above inhibitors. The estimated K_i based on Eqs. 13-15 for sodium azide, 2,4-dinitrophenol, verapamil was 8.8 mM, 1.5 mM, and 6.8 μM, respectively. However, probenecid, MK-571 and celecoxib slightly altered the AP-BL and BL-AP P_{app} values ($P > 0.05$), suggesting that MRPs play a minor or negligible role in the intestinal transport of glabridin.

Uptake and Efflux of Glabridin in Control MDCKII and MDR1-MDCKII Cells

As shown in **Figure 8**, the intracellular accumulation and efflux amounts of glabridin in both control MDCKII and MDR1-MDCKII cells were linear up to 120 min of

DMD Fast Forward. Published on January 12, 2007 as DOI: 10.1124/dmd.106.010801
This article has not been copyedited and formatted. The final version may differ from this version.

incubation time. The accumulation and efflux rate of glabridin in both control MDCKII and MDR1-MDCKII cells over 0.1–50 μM increased in a concentration-dependent manner, following the Michaelis-Menten kinetics with the one-binding site model the best fit (**Figure 8**). The estimated K_m and V_{max} in both control MDCKII and MDR1-MDCKII cells for glabridin uptake were 12.75 ± 1.43 and 10.91 ± 2.23 μM; and 16.22 ± 0.70 and 4.47 ± 0.34 ng/min/mg cellular proteins, respectively (**Figure 8**). The uptake of glabridin by control MDCKII cell was significantly (about 3-fold) higher than that in MDR1-MDCKII cells ($P < 0.05$). The estimated K_m and V_{max} in both control MDCKII and MDR1-MDCKII cells were 5.70 ± 1.75 and 5.60 ± 0.73 μM; and 8.44 ± 0.81 and 60.03 ± 2.44 pg/min/mg cellular proteins, respectively. The efflux rate of glabridin from MDR1-MDCKII cell was significantly (about 5- to 7-fold) higher than that in control MDCKII cells ($P < 0.05$ or < 0.01).

These results suggest that PgP/MDR1 diminished the uptake and increased the efflux of glabridin by MDCKII cells and glabridin is likely a substrate for PgP/MDR1. Nevertheless, the diminished accumulation and increased efflux in MDR1-MDCKII cells compared to the control MDCKII cells cannot be attributable to drug-induced plasma membrane damage, which in turn could cause cellular leakage and increase drug influx and efflux. The cells remained viable during drug accumulation studies over 120 min as measured using trypan blue exclusion.

DMD Fast Forward. Published on January 12, 2007 as DOI: 10.1124/dmd.106.010801
This article has not been copyedited and formatted. The final version may differ from this version.

Uptake of the probe markers sucrose and propranolol into both control MDCKII and MDR1-MDCKII cells was also determined upon incubation up to 120 min. Propranolol penetrated into both cell lines to a low degree with a value of 0.18 ± 0.02 – 0.37 ± 0.40 ng/min/mg cellular protein, and diffusion of sucrose into the cells was minimal (0.03 ± 0.00 – 0.06 ± 0.01 ng/min/mg cellular protein). The uptake of sucrose and propranolol did not increase with incubation time and substrate concentration in both cell lines. These findings indicate that PgP/MDR1 did not significantly affect the uptake of both sucrose and propranolol. In addition, the efflux of the probe drug, vinblastine, from MDR1-MDCKII cell was significantly (about 4- to 8-fold) higher than that in control MDCKII cells (data not shown).

Transport of Glabridin in Control MDCKII and MDR1-MDCKII Monolayers

To further investigate the nature of the polarized transport of glabridin, transport studies were conducted in control MDCKII and MDR1-MDCKII cells which stably and functionally over-express the human PgP/MDR1. Our Western blotting analysis demonstrated that control MDCKII cells expressed constitutive canine P-glycoprotein at a much lower level to that in the recombinant MDR1-MDCKII cells (data not shown).

The transport data across these two MDCKII cell lines for glabridin are shown in **Figure 9**. Consistent with the data for glabridin in the Caco-2 monolayer studies, glabridin at 0.1–50 μM in the control MDCKII monolayers showed a significantly (*P*

DMD Fast Forward. Published on January 12, 2007 as DOI: 10.1124/dmd.106.010801
This article has not been copyedited and formatted. The final version may differ from this version.

< 0.05, or 0.01) greater (about 2-fold) permeability in BL-AP direction compared to that in the AP-BL direction. The transport of glabridin across MDR1-MDCKII monolayers was also examined and compared with the control cells. Most apparent is that the extent of polarized transport is now more profound, with R_{net} values for glabridin ranging from 9.0–20.1.

At all substrate concentrations, the permeability of glabridin in the BL-AP direction in the MDR1-MDCKII cells were significantly ($P < 0.01$ or 0.001) greater than that in the BL-AP direction in control MDCKII cells. As for the Caco-2 data, increased glabridin concentration also resulted in lower P_{app} values in both AP-BL and BL-AP directions for both MDCKII and MDR1-MDCKII monolayers.

Inhibition of P-glycoprotein-Mediated Digoxin Transport by Glabridin

We examined the effects of glabridin on PgP-mediated transport of the probe digoxin in Caco-2 monolayers. The results are shown in **Figure 10**. Glabridin inhibited digoxin transport in a concentration-dependent manner with an IC_{50} value of 2.56 ± 0.04 μM. In addition, verapamil exhibited potent inhibitory effects on PgP-mediated transport of digoxin, with an IC_{50} value of 2.34 ± 0.03 μM. These results indicated that glabridin was a potent PgP inhibitor *in vitro*.

Stimulation of P-glycoprotein ATPase Activity by Glabridin

The affinity of glabridin to PgP/MDR1 was assessed by ATPase activity assay. The

DMD Fast Forward. Published on January 12, 2007 as DOI: 10.1124/dmd.106.010801
This article has not been copyedited and formatted. The final version may differ from this version.

plot of ATP hydrolysis as a function of glabridin concentrations over 0.1–100 μM demonstrated a concentration-dependent stimulation of vanadate-sensitive PgP/MDR1 ATPase activity (**Figure 11**). The one-binding site model was the best fit for this reaction. The estimated K_m and V_{max} values of PgP/MDR1-mediated ATP hydrolysis by glabridin were 25.05 ± 2.86 μM and 80.50 ± 3.47 nmol/min/mg protein, respectively. In addition, a significant stimulatory effect was exhibited by verapamil over 0.25–100 μM with a K_m and V_{max} of 5.98 ± 0.7 μM and 89.34 ± 2.84 nmol/min/mg protein, respectively. The estimated K_m value for verapamil to PgP/MDR1-mediate ATP hydrolysis was in agreement with previously reported values (4.06–6.10 μM) (Adachi et al., 2001; Ohashi et al., 2006).

Effect of Coadministered Verapamil on the Plasma Pharmacokinetics of Glabridin in Rats

The plasma concentration-time profiles when glabridin was coadministered alone or in combination with verapamil at 25 or 100 mg/kg are shown in **Figure 12** and the pharmacokinetic parameters are shown in TABLE 3. Combined verapamil significantly (P <0.05) increased the plasma C_{max} and $AUC_{0\text{-}24h}$ of glabridin in a dose-dependent manner. Co-administered verapamil at 25 and 100 mg/kg caused a significant increase (P < 0.05) in plasma C_{max} [from 15.02 ± 4.59 (control) to 19.01 ± 5.38 and 25.38 ± 7.62 ng/ml, respectively] and $AUC_{0\text{-}24h}$ [from 97.41 ± 34.58 (control) to 116.21 ± 36.36 and 170.52 ± 52.28 ng/ml•h, respectively], compared to the control rats receiving glabridin alone. The oral bioavailability of glabridin was

DMD Fast Forward. Published on January 12, 2007 as DOI: 10.1124/dmd.106.010801
This article has not been copyedited and formatted. The final version may differ from this version.

correspondingly increased from 7.55% to 9.02% and 13.19%, respectively. In addition, coadministered verapamil increased the $t_{1/2\beta}$ values of glabridin in a dose-dependent manner. Furthermore, the T_{max} of glabridin was 4.15 ± 0.97 h, whereas it was significantly ($P < 0.05$) decreased to 2.25 ± 0.52 and 2.15 ± 0.46 h when glabridin was coadministered with 25 and 100 mg/kg verapamil, respectively.

A Comparison of Plasma Pharmacokinetics of Glabridin in *mdr1a(-/-)*and Wildtype Mice

To further investigate the impact of PgP/MDR1 on the plasma pharmacokinetics, we compared the pharmacokinetics of glabridin in *mdr1a*(-/-) and wilt-type mice. The results are shown in **Figure 13** and TABLE 4. The plasma pharmacokinetics of glabridin in *mdr1a*(-/-) mice were significantly different from those in wildtype mice. The plasma $AUC_{0\text{-}24h}$ and C_{max} of glabridin in *mdr1a*(-/-) mice were 3.77- and 2.83-fold higher than that in wildtype mice, respectively, with significantly longer elimination half-life observed in *mdr1a*(-/-) mice compared to wildtype mice (3.54 ± 1.14 vs 2.97 ± 0.89 h). These findings provided further evidence that PgP/MDR1 had an important impact to the oral bioavailability and elimination *in vivo*.

DMD Fast Forward. Published on January 12, 2007 as DOI: 10.1124/dmd.106.010801
This article has not been copyedited and formatted. The final version may differ from this version.

DISCUSSION:

The systemic bioavailability of glabridin after oral administration at 5 and 20 mg/kg was very low (about 7.5%). Moderate to high plasma clearance (59.0 ml/min/kg) of glabridin was observed in rats, which was partially attributed to partitioning into red blood cells based on an approximate blood:plasma concentration ratio of 1.6 (Unpublished data, Huang M, X Chen & Zhou SF). Therefore, blood clearance of glabridin was 1.6-fold lower than plasma clearance and was approximately 43% of hepatic blood-flow in rats (approximately 85.0 ml/min/kg). If glabridin was well absorbed and cleared mainly in the liver, its oral bioavailability would be expected to be about 57% calculated from 100% minus 43%.

Microsomal study demonstrated that glabridin was extensively glucuronidated in the liver. To a much lesser extent, the intestine could also metabolize glabridin by glucuronidation. The low water solubility of glabridin, intestinal transporter-mediated efflux, and first-pass metabolism are considered the major factors for its low oral bioavailability.

The absorption of glabridin in the single-pass perfused rat ileum was monitored by determination of disappearance permeability (P_{lumen}) and appearance permeability (P_{blood}). The P_{lumen} for glabridin ($6.51–11.54 \times 10^{-4}$ cm/sec at substrate concentrations of 0.1–2.0 μM) was higher than that of verapamil (3.07×10^{-5} cm/sec) (Johnson et al., 2003), lidocaine (7.5×10^{-5} cm/sec) (Berggren et al., 2004), and RU60079 (a novel

DMD Fast Forward. Published on January 12, 2007 as DOI: 10.1124/dmd.106.010801
This article has not been copyedited and formatted. The final version may differ from this version.

angiotensin II antagonist, 1.4×10^{-6} cm/sec) (Boisset et al., 2000), but lower than warfarin (7.7×10^{-3} cm/min) (Okudaira et al., 2000). The much lower P_{blood} (about 7-fold) than P_{lumen} of glabridin indicated extensive intestinal efflux and/or gut metabolism. Such marked difference between P_{blood} and P_{lumen} occurs because permeability calculations based only on drug disappearance from the lumen cannot distinguish drug losses due to absorption from that due to extensive gut metabolism (Dackson et al., 1992). These data also illustrated the potentially different conclusions that might be drawn as to the importance of PgP/MDR1 efflux on drug absorption when evaluating permeability based on drug disappearance as opposed to drug appearance values in the single pass intestinal perfusion model.

There was only minimal metabolite formation detected using LC-MS analysis in the perfusates or mesenteric vein blood when glabridin was loaded, suggesting that extensive metabolism of glabridin in the gut did not occur. The lack of effect of verapamil on P_{lumen} but P_{blood} instead was considered due to the PgP/MDR1 inhibition, rather than inhibition of intestinal first-pass metabolism. A lack of effect of verapamil on P_{lumen} was also found in previous studies with verapamil (Sandstrom et al., 1999; Johnson et al., 2003). PSC833, a known potent PgP/MDR1 inhibitor, significantly increased the P_{blood} of verapamil, but insignificantly affected its disappearance in perfused rat jejunum (Johnson et al., 2003). Similar results were observed with verapamil in the presence of ketoconazole (a known potent cytochrome P450 3A4 and PgP/MDR1 inhibitor) in a human intestinal perfusion study (Sandstrom et al., 1999).

DMD Fast Forward. Published on January 12, 2007 as DOI: 10.1124/dmd.106.010801
This article has not been copyedited and formatted. The final version may differ from this version.

These findings most likely reflected the small impact of PgP/MDR1-mediated efflux on the disappearance of glabridin in the lumen and thus verapamil had minor effect on the permeability of glabridin. Substantial tissue uptake and binding of both substrate and potential inhibitors could also compromise the effect of PgP inhibitors.

The uptake and efflux assays of glabridin in Caco-2 cells were conducted under non-sink conditions. Under such non-sink conditions, the efflux of glabridin from Caco-2 cells followed a one-phase exponential kinetics, which reflected that the efflux process was entirely driven by passive diffusion. The intracellular accumulation of glabridin in Caco-2, control MDCKII and MDR1-MDCKII cells was investigated in this study. The uptake of glabridin in these cells was different with different uptake rates. This may be due mainly to the different biological properties of these cell lines, for example, the differential nature of tight junctions, cellular membrane and other factors, resulting in differential uptake rate. However, the K_m values for all these cell lines are similar ranging from 10.91 to 12.75 μM, indicating similar mechanism of passive diffusion for glabridin under non-sink condition in all these cells.

However, the observed difference in the estimated K_m for glabridin uptake and efflux (12.38 ± 1.41 vs 4.68 ± 1.03 μM) indicated the presence of an active transport mechanism because for a compound entirely driven by passive diffusion, the affinities for uptake and efflux would not be expected to differ. Therefore, both active and passive transport were likely involved in the uptake and efflux of glabridin by the

cells tested. A number of flavonoids can be readily taken up and pumped out by human Caco-2 and other tumor cells through active (may involve PgP/MDR1 and MRPs) and/or passive diffusion (Zhou et al., 2004). PgP is highly likely to be involved in the influx and efflux of glabridin in these types of cells, as indicated by the significant enhanced accumulation and decreased efflux of the substrate in the presence of nifedipine or verapamil (both PgP inhibitors). Glabridin appeared to enter these cells at a rapid rate, but the exact process of how cells dispose glabridin is unclear.

Like glabridin, the P_{app} for BL-AP or AP-BL flux decreased with increasing substrate concentration for many compounds such as cryptotanshinone (a major active constituent of *Salvia miltiorrhiza*) (Zhang et al., 2006) and several aryloxy phosphoramidate derivatives (all PgP/MDR1 substrates) of the anti-HIV agent stavudine (Siccardi et al., 2003). This may reflect that P_{app} is affected by a number of factors associated with the intestine and drugs, in particular for substrates with some intrinsic permeability and substantial tissue uptake and binding.

We found that the permeability of the Caco-2 monolayers to glabridin is nonlinear over the concentrations of 0.1–50 μM. The deviation from linearity suggests the presence of a polarized efflux pump and/or a saturable metabolic barrier to absorption. However, the intrinsic permeabilities of glabridin in Caco-2 and MDCKII monolayers compared to most lipophilic drugs and negligible metabolite (glucuronide) formation

in Caco-2 cells indicated that the first-pass metabolism within the enterocytes played a minor role in limiting the oral absorption of glabridin. The increased glabridin permeability in apical to basolateral direction in Caco-2 monolayers by coincubated verapamil was considered due to inhibition of PgP/MDR1 instead of glabridin metabolic inhibition. The permeability data from the single-pass intestinal perfusion model and Caco-2 monolayers (TABLE 2 & **Figure 5**) provided initial evidence that PgP-mediated efflux into the luminal side might play an important role in the low oral bioavailability of glabridin in rats and in humans, providing that there are no species differences with regards to the rate and extent of active transport and intestinal metabolism of glabridin.

The permeability coefficients for AP-BL transport of glabridin in Caco-2 monolayers (**Figure 5**) were about 3.3 to 8.4 folds lower than those in the BL-AP direction. A significant increase in the AB-BL flux of glabridin in the presence of sodium azide at 10 mM or 2,4-dinitrophenol at 5 mM provided supportive evidence for the involvement of an ATP-dependent active mechanism for glabridin intestinal transport. Furthermore, the addition of the PgP inhibitor verapamil markedly reduced the transport of glabridin in the BL-AP direction. However, the MRP inhibitors, probenecid, MK-571 and celecoxib, had insignificant effect on glabridin transport in Caco-2 monolayers, excluding glabridin as a substrate for MRP1-4.

Transport data in the MDCKII and MDR1-MDCKII model further provided evidence

that glabridin was a substrate for PgP. Glabridin was significantly more permeable in the BL-AP direction than in the AP-BL direction in both cell lines. The permeability coefficients in the BL-AP direction were significantly higher in the cell line over-expressing PgP (**Figure 9**). In addition, the uptake and efflux of glabridin by control MDCKII cells were significantly different from those values observed in MDR1-MDCKII cells, and this difference could be significantly altered in the presence of PgP inhibitors. This provided additional evidence supporting our hypothesis.

Many PgP/MDR1 substrates are also PgP/MDR1 inhibitors or modulators. Thus, we examined the effect of glabridin on PgP/MDR1-mediated transport of digoxin using Caco-2 models. The observed IC_{50} value (2.34 μM) for glabridin indicated that glabridin was a potent inhibitor for PgP/MDR1 compared to many other reported potent PgP inhibitors such as ketoconazole (1.2 μM) and cyclosporine (1.3 μM) when using the translocation of digoxin across Caco-2 cells as the model (Choo et al., 2000). The observed IC_{50} value for verapamil (2.57 μM) in this study is similar to those reported by other groups (Choo et al., 2000). In addition, we found glabridin stimulated PgP/MDR1 ATPase activity with a K_m of 25.1 μM, suggesting that glabridin as a modulator has moderate affinity to PgP/MDR1 protein. This may provide some insight into the mechanism for the inhibition of PgP/MDR1-mediated digoxin transport by glabridin. It would be interesting to investigate how glabridin interacts with the ATP binding sites of PgP/MDR1 and affects its hydrolysis.

DMD Fast Forward. Published on January 12, 2007 as DOI: 10.1124/dmd.106.010801
This article has not been copyedited and formatted. The final version may differ from this version.

Results from the present study suggested that PgP/MDR1 played a major role in the intestinal transport of glabridin, but the contribution of MDR3 cannot be excluded. Not all these proteins confer resistance to drugs; transfection experiments have shown that the expression of human PgP/MDR1 or rodent mdr1a or mdr1b is sufficient to confer resistance to anticancer agents, whereas MDR3 (ABCB4) and mdr2 are involved in the transport of other molecules, such as phospholipids in the bile (Borst and Elferink, 2002). The role of MDR3 for intestinal transport of drugs is likely to be minor because MDR3 is expressed in the canalicular membrane of hepatocytes, heart, muscle and B-cells but not in the intestine, whereas in the intestine MDR3 transcripts were only detected at a very low level (Taipalensuu et al., 2001). MDR1-mediated drug-drug interactions have been reported, drug interaction studies of glabridin with PgP/MDR1 substrates/inhibitors should be considered in future clinical trials.

To further address the role of PgP/MDR1 in the in vivo disposition of glabridin, we examined the effects of coadministered verapamil on the systemic bioavailability and plasma pharmacokinetics of glabridin. Verapamil significantly increased the oral bioavailability of glabridin in rats. Similar results in rats have been observed with colchicine or vinblastine as the substrate and verapamil as the inhibitor (Drion et al., 1996). In the same way, SDZ PSC 833, a potent PgP inhibitor, also significantly increased the systemic bioavailability of cyclosporine and vincristine in rats (Lemaire et al., 1996). Inhibition of intestinal PgP/MDR1 was considered one of the major

reasons for increased oral bioavailability of glabridin by combined verapamil. A significantly increased half-lives of glabridin by coadministered verapamil indicated that verapamil might inhibit PgP/MDR1-mediated hepato-biliary and renal efflux of glabridin. Because glabridin has a low molecular weight (354 Dalton) and high lipophilicity, the most likely mechanism for its hepato-biliary and renal efflux would be a transporter-mediated process. Clearance of PgP substrates through biliary and/or renal secretion can be significantly decreased in the presence of a PgP inhibitor (Song et al., 1999). The localization of the protein also suggests that the function of PgP/MDR1 is related to transport mechanism of glabridin in the liver and kidneys because there are high levels of PgP/MDR1 protein in the brush border of renal proximal tubules and biliary surface of hepatocytes. However, it should be noted that verapamil might have other effects rather than PgP inhibition that lead to altered pharmacokinetics of PgP/MDR1 substrates.

The comparative study in *mdr1a(-/-)* and wildtype mice indicated that depletion of PgP *in vivo* significantly increased the oral bioavailability and elimination half-life of glabridin. This provided further evidence that PgP/MDR1 had an important impact to the oral bioavailability and elimination *in vivo*.

Because our *in vitro* experiments indicated that glabridin only underwent minimal glucuronidation in rat intestinal microsomes and verapamil did not alter glabridin metabolism in the intestine, the significant inhibition of intestinal PgP/MDR1 by

DMD Fast Forward. Published on January 12, 2007 as DOI: 10.1124/dmd.106.010801
This article has not been copyedited and formatted. The final version may differ from this version.

verapamil would not decrease intestinal glabridin first-pass metabolism in a synergistic manner. Such effect would not been seen *in vivo* using a multipsecific inhibitor such as verapamil or cyclosporine. A combined use of specific inhibitors such as elacridar/zosquidar with a multispecific, i.e. PgP and cytochrome P450 3A4 inhibitor such as cyclosporine can provide an insight into the role of PgP on drug intestinal absorption and first-pass metabolism (Cummins et al., 2002).

Identification of glabridin as a PgP substrate, low intestinal first-pass metabolism which could not be inhibited by verapamil and a marked shift in T_{max} after coadministration of glabridin as well as the data obtained from the perfusion experiments indicated that both PgP-mediated efflux and first-pass metabolism contribute to the low oral bioavailability of glabridin in rats.

In conclusion, glabridin has a low oral bioavailability in rats. Glabridin is a substrate and an inhibitor for PgP/MDR1. PgP-mediated active efflux across the intestine partly contributed to the low bioavailability of glabridin, as indicated by the verapamil-glabridin interactions *in vitro* and *in vivo* and the findings from the comparative study in *mdr1a(-/-)* and wildtype mice. First-pass metabolism is also considered to play an important role for a low oral bioavailability of glabridin. Further research addressing the role of PgP/MDR1 and other transporters in the disposition and *in vivo* distribution of glabridin is warranted.

REFERENCES:

Adachi Y, Suzuki H and Sugiyama Y (2001) Comparative studies on in vitro methods for evaluating in vivo function of MDR1 P-glycoprotein. *Pharm Res* **18:**1660-1668.

Belinky PA, Aviram M, Fuhrman B, Rosenblat M and Vaya J (1998) The antioxidative effects of the isoflavan glabridin on endogenous constituents of LDL during its oxidation. *Atherosclerosis* **137:**49-61.

Berggren S, Hoogstraate J, Fagerholm U and Lennernas H (2004) Characterization of jejunal absorption and apical efflux of ropivacaine, lidocaine and bupivacaine in the rat using in situ and in vitro absorption models. *Eur J Pharm Sci* **21:**553-560.

Boisset M, Botham RP, Haegele KD, Lenfant B and Pachot JI (2000) Absorption of angiotensin II antagonists in Ussing chambers, Caco-2, perfused jejunum loop and in vivo: importance of drug ionisation in the in vitro prediction of in vivo absorption. *Eur J Pharm Sci* **10:**215-224.

Borst P and Elferink RO (2002) Mammalian ABC transporters in health and disease. *Annu Rev Biochem* **71:**537-592.

Choo EF, Leake B, Wandel C, Imamura H, Wood AJ, Wilkinson GR and Kim RB (2000) Pharmacological inhibition of P-glycoprotein transport enhances the distribution of HIV-1 protease inhibitors into brain and testes. *Drug Metab Dispos* **28:**655-660.

Cummins CL, Jacobsen W and Benet LZ (2002) Unmasking the dynamic interplay between intestinal P-glycoprotein and CYP3A4. *J Pharmacol Exp Ther* **300:**1036-1045.

Dackson K, Stone JA, Palin KJ and Charman WN (1992) Evaluation of the mass balance assumption with respect to the two-resistance model of intestinal absorption by using in situ single-pass intestinal perfusion of theophylline in rats. *J Pharm Sci* **81:**321-325.

Drion N, Lemaire M, Lefauconnier JM and Scherrmann JM (1996) Role of P-glycoprotein in the blood-brain transport of colchicine and vinblastine. *J Neurochem* **67:**1688-1693.

El Hafny B, Cano N, Piciotti M, Regina A, Scherrmann JM and Roux F (1997) Role of P-glycoprotein in colchicine and vinblastine cellular kinetics in an immortalized rat brain microvessel endothelial cell line. *Biochem Pharmacol* **53:**1735-1742.

Fromm MF (2004) Importance of P-glycoprotein at blood-tissue barriers. *Trends Pharmacol Sci* **25:**423-429.

Hayashi H, Hattori S, Inoue K, Khodzhimatov O, Ashurmetov O, Ito M and Honda G (2003) Field survey of Glycyrrhiza plants in Central Asia (3). Chemical characterization of G. glabra collected in Uzbekistan. *Chem Pharm Bull (Tokyo)* **51:**1338-1340.

Hung DY, Chang P, Weiss M and Roberts MS (2001) Structure-hepatic disposition relationships for cationic drugs in isolated perfused rat livers: transmembrane

exchange and cytoplasmic binding process. *J Pharmacol Exp Ther* **297:**780-789.

Johnson BM, Chen W, Borchardt RT, Charman WN and Porter CJ (2003) A kinetic evaluation of the absorption, efflux, and metabolism of verapamil in the autoperfused rat jejunum. *J Pharmacol Exp Ther* **305:**151-158.

Kunta JR and Sinko PJ (2004) Intestinal drug transporters: in vivo function and clinical importance. *Curr Drug Metab* **5:**109-124.

Lemaire M, Bruelisauer A, Guntz P and Sato H (1996) Dose-dependent brain penetration of SDZ PSC 833, a novel multidrug resistance-reversing cyclosporin, in rats. *Cancer Chemother Pharmacol* **38:**481-486.

Miki K, Butler R, Moore D and Davidson G (1996) Rapid and simultaneous quantification of rhamnose, mannitol, and lactulose in urine by HPLC for estimating intestinal permeability in pediatric practice. *Clin Chem* **42:**71-75.

Ohashi R, Kamikozawa Y, Sugiura M, Fukuda H, Yabuuchi H and Tamai I (2006) Effect of P-glycoprotein on intestinal absorption and brain penetration of anti-allergic agent bepotastine besilate. *Drug Metab Dispos* **Published online**.

Okudaira N, Tatebayashi T, Speirs GC, Komiya I and Sugiyama Y (2000) A study of the intestinal absorption of an ester-type prodrug, ME3229, in rats: active efflux transport as a cause of poor bioavailability of the active drug. *J Pharmacol Exp Ther* **294:**580-587.

Rosenblat M, Belinky P, Vaya J, Levy R, Hayek T, Coleman R, Merchav S and Aviram M (1999) Macrophage enrichment with the isoflavan glabridin

inhibits NADPH oxidase-induced cell-mediated oxidation of low density lipoprotein. A possible role for protein kinase C. *J Biol Chem* **274:**13790-13799.

Sandstrom R, Knutson TW, Knutson L, Jansson B and Lennernas H (1999) The effect of ketoconazole on the jejunal permeability and CYP3A metabolism of (R/S)-verapamil in humans. *Br J Clin Pharmacol* **48:**180-189.

Siccardi D, Kandalaft LE, Gumbleton M and McGuigan C (2003) Stereoselective and concentration-dependent polarized epithelial permeability of a series of phosphoramidate triester prodrugs of d4T: an in vitro study in Caco-2 and Madin-Darby canine kidney cell monolayers. *J Pharmacol Exp Ther* **307:**1112-1119.

Smith PK, Krohn RI, Hermanson GT, Mallia AK, Garter FH, Provenzano MD, Fujimoto EK, Goeke NM, Olson BJ and Klenk DC (1985) Measurement of protein using bicinchoninic acid. *Anal Biochem* **150:**76-85.

Song S, Suzuki H, Kawai R and Sugiyama Y (1999) Effect of PSC 833, a P-glycoprotein modulator, on the disposition of vincristine and digoxin in rats. *Drug Metab Dispos* **27:**689-694.

Taipalensuu J, Tornblom H, Lindberg G, Einarsson C, Sjoqvist F, Melhus H, Garberg P, Sjostrom B, Lundgren B and Artursson P (2001) Correlation of gene expression of ten drug efflux proteins of the ATP-binding cassette transporter family in normal human jejunum and in human intestinal epithelial Caco-2 cell monolayers. *J Pharmacol Exp Ther* **299:**164-170.

Tamir S, Eizenberg M, Somjen D, Stern N, Shelach R, Kaye A and Vaya J (2000) Estrogenic and antiproliferative properties of glabridin from licorice in human breast cancer cells. *Cancer Res* **60:**5704-5709.

Vaya J, Belinky PA and Aviram M (1997) Antioxidant constituents from licorice roots: isolation, structure elucidation and antioxidative capacity toward LDL oxidation. *Free Radic Biol Med* **23:**302-313.

Yamaoka K, Nakagawa T and Uno T (1978) Application of Akaike's information criterion (AIC) in the evaluation of linear pharmacokinetic equations. *J Pharmacokinet Biopharm* **6:**165-167.

Yokota T, Nishio H, Kubota Y and Mizoguchi M (1998) The inhibitory effect of glabridin from licorice extracts on melanogenesis and inflammation. *Pigment Cell Res* **11:**355-361.

Zhang J, Huang M, Guan S, Bi HC, Pan Y, Duan W, Chan SY, Chen X, Hong YH, Bian JS, Yang HY and Zhou SF (2006) A mechanistic study of the intestinal absorption of cryptotanshinone, the major active constituent of *Salvia miltiorrhiza*. *J Pharmacol Exp Ther* **317:**1285-1294.

Zhou S, Feng X, Kestell P, Paxton JW, Baguley BC and Chan E (2005) Transport of the investigational anti-cancer drug 5,6-dimethylxanthenone-4-acetic acid and its acyl glucuronide by human intestinal Caco-2 cells. *Eur J Pharm Sci* **24:**513-524.

Zhou S, Lim LY and Chowbay B (2004) Herbal modulation of P-glycoprotein. *Drug Metab Rev* **36:**57-104.

Zhou S, Paxton JW, Tingle MD and Kestell P (2000) Identification of the human liver cytochrome P450 isoenzyme responsible for the 6-methylhydroxylation of the novel anticancer drug 5,6-dimethylxanthenone-4-acetic acid. *Drug Metab Dispos* **28:**1449-1456.

Zhu Y-P (1998) *Chinese materia medica: chemistry, pharmacology and applications*. Harwood Academic Publishers, Amsterdam, The Netherlands.

DMD Fast Forward. Published on January 12, 2007 as DOI: 10.1124/dmd.106.010801
This article has not been copyedited and formatted. The final version may differ from this version.

FOOTNOTES SECTION:

a) The authors appreciate the financial support provided by the Australia Institute of Traditional Chinese Medicine (Grant Nos. R-106-00257 & R-106-00282).

b) These three authors (Cao J, Chen X & Liang J) contributed equally to this work.

c) Person to receive reprint request

Dr Shu-Feng Zhou, MD, PhD

Department of Pharmacology and Toxicology, Australian Institute of Chinese Medicine, 167 Pennant Hills Road, Carlingford, New South Wales 2118, Australia.

Tel: 0061 2 88122471; Fax: 00612 88123472

Email: shufengzhou2006@hotmail.com

FIGURE LEGENDS:

Figure 1. Chemical structures of glabridin and mefenamic acid.

Figure 2. The representative plasma concentration-time profiles of glabridin after oral administration at 5 and 20 mg/kg and intravenous bolus injection at 5 mg/kg (n = 6 per group).

Figure 3. Effects of incubation time (A & C) and substrate concentration (B & D) on the uptake and efflux of glabridin in Caco-2 cells cultured in HBSS. The curves in plots B & D represent the best fit of one binding-site model. (E) The kinetic profiles of glabridin efflux from Caco-2 cells when preloaded at 1.0 μM and the intracellular concentrations of glabridin were monitored by LC-MS over 120 min of incubation. The data are the mean ± SD of at least 6-9 determinations.

Figure 4. Effects of sodium azide, 2,4-dinitrophenol, verapamil, nifedipine, probenecid, MK-571 and celecoxib on the uptake (A) in Caco-2 cells and efflux (B) of glabridin at 1.0 μM from Caco-2 cells upon pre-incubation with the inhibitor for 2 h followed by 30 min incubation with the substrate. The data are the mean ± SD of at least 6-9determinations. *$P < 0.05$; **$P < 0.01$.

Figure 5. Transport of glabridin across Caco-2 monolayers. (A) Effect of

concentration of glabridin (0.1–50 μM) on the permeability (P_{app}) of glabridin from apical (AP) to basolateral (BL) and BL to AP side; and (B) Effect of incubation time (0–60 min) on the permeability (P_{app}) of glabridin at 1.0 μM in the AP to BL and BL-AP directions. Glabridin was loaded on either AP or BL side and incubated at 37°C. Samples from receiving side were collected at indicated time points and glabridin was determined by LC-MS. Data are the mean ± SD from at least 6-9 determinations. $^{**}P < 0.01$.

Figure 6. Model fitting for the passive and active transport of glabridin from apical (AP) to basolateral (BL) and BL to AP sides in Caco-2 monolayers. The passive and active BL-AP and AP-BL transport was calculated only based on verapamil inhibition of PgP in Caco-2 cells assuming that the role of other transporters is minimal and ignored. Glabridin (0.1–50 μM) was loaded on either AP or BL side and incubated at 37°C over 30 min. Samples from receiving side were collected and glabridin was determined by LC-MS. Data are the mean ± SD from independent 6-9 determinations. The curve represents the best fit of one saturable transport model.

Figure 7. Effect of various inhibitors, including sodium azide (10 mM), 2,4-dinitrophenol (5 mM), verapamil (100 μM), probenecid (200 μM), MK-571 (100 μM) and celecoxib (100 μM) on the apical (AP) to basolateral (BL) and BL to AP transport of glabridin at 0.1 μM (A) or 1.0 μM (B) in Caco-2 monolayers upon incubation for 30 min. Glabridin (0.1 or 1.0 μM) was loaded on either apical or

basolateral side and incubated for 30 min at 37°C. Transport studies were undertaken in the absence or presence of the potential inhibitor added to both the apical and basal compartments. Samples from receiving side were collected and glabridin concentrations were determined by LC-MS methods. Data are the mean ± SD from at least 6-9 determinations. *$P < 0.05$; **$P < 0.01$.

Figure 8. Effects of incubation time (A & C) and substrate concentration (B & D) on the uptake and efflux of glabridin in control MDCKII and MDR1-MDCKII cells cultured in HBSS. The curves in plots B & D represent the best fit of one binding-site model. The data are the mean ± SD of at least 6-9 determinations. *$P < 0.05$; **$P < 0.01$.

Figure 9. Transport of glabridin (0.1–50 μM) from apical (AP) to basolateral (BL) and BL to AP side in control MDCKII and MDR1-MDCKII monolayers. Glabridin was loaded on either AP or BL side and incubated at 37°C for 15 min. Samples from receiving side were collected at indicated time points and glabridin was determined by LC-MS. Data are the mean ± SD from at least 6-9 determinations. **$P < 0.01$; ***$P < 0.001$.

Figure 10. Effects of glabridin on the transport of digoxin in Caco-2 monolayers. The transport of [^{3}H]-digoxin at 5.0 μM (15 Ci/mmol) was determined by its addition to the basolateral (BL) side of the Caco-2 monolayer and by measuring the transport of

DMD Fast Forward. Published on January 12, 2007 as DOI: 10.1124/dmd.106.010801
This article has not been copyedited and formatted. The final version may differ from this version.

radioactivity in the other compartment (apical side) over 1 h, in the absence or presence of glabridin (0.1–200 μM), or verapamil (0.25–50 μM), added in both sides. $^{**}P < 0.01$.

Figure 11. Concentration-dependent stimulation of P-glycoprotein (PgP) ATPase activity in isolated membrane fractions from human MDR1 expressing cells by glabridin (A) and verapamil (B). The ATPase activity in PgP membrane was determined by measuring vanadate-sensitive inorganic phosphate release, using 4 mM MgATP, as described in *Materials and Methods*. Data are the mean ± SD from at least 3 independent experiments. The vanadate-sensitive ATP hydrolysis was determined by subtracting the values obtained with the vanadate co-incubated PgP membrane fractions from vanadate-free membrane fractions. One-binding site model is the best fit for the ATP hydrolysis reaction stimulated by both glabridin and verapamil. $^{*}P < 0.05$; $^{**}P < 0.01$.

Figure 12. The plasma concentration-time profiles in rats treated with glabridin alone or glabridin in combination with 5 or 25 mg/kg verapamil dosed orally. Rats were treated with glabridin at 5 mg/kg by gavage and the plasma concentrations of glabridin over 24 h were determined by LC-MS analysis. Data are the mean ± SD of 6 rats.

Figure 13. The plasma concentration-time profiles of glabridin in *mdr1a(-/-)* and

DMD Fast Forward. Published on January 12, 2007 as DOI: 10.1124/dmd.106.010801
This article has not been copyedited and formatted. The final version may differ from this version.

wildtype mice. Mice were treated with glabridin at 5 mg/kg by gavage and the plasma concentrations of glabridin over 24 h were determined by LC-MS analysis. Data are the mean ± SD of 4 mice per time point.

DMD Fast Forward. Published on January 12, 2007 as DOI: 10.1124/dmd.106.010801
This article has not been copyedited and formatted. The final version may differ from this version.

TABLES:

TABLE 1. The pharmacokinetics parameters (n = 6) of glabridin after oral (p.o.), at 5 and 20 mg/kg and intravenous (i.v.) bolus injection at 5 mg/kg.

Parameter[a]	p.o. (5 mg/kg)	p.o. (20 mg/kg)	i.v. (5 mg/kg)
T_{max} (h)	4.33 ± 1.86	4.50 ± 2.17	NC
C_{max} (ng/ml)	15.10 ± 4.72	60.41 ± 18.87	422.96 ± 123.92
$t_{1/2\beta}$ (h)	2.38 ± 0.70	2.41 ± 0.74	1.92 ± 0.60
$AUC_{0\text{-}24hr}$ (ng/ml•h)	96.49 ± 32.34	387.98 ± 137.28	1301.48 ± 375.79
$AUC_{0\text{-}\infty}$ (ng/ml•h)	103.54 ± 34.03	413.30 ± 127.72	1388.49 ± 400.22
CL (ml/min/kg)	NC	NC	59.01
V_d (L/kg)	NC	NC	2.72
F	7.45%	7.44%	NC

Data are the mean ±SD. NC = Not calculated.

[a]Parameters calculated: T_{max} = Time to maximum plasma concentration; C_{max} = maximum plasma concentration; $t_{1/2\beta}$ = elimination half-life; AUC = the area under the plasma concentration time curve; CL = plasma clearance; V_d = volume of distribution; and F = systemic bioavailability after oral administration.

DMD Fast Forward. Published on January 12, 2007 as DOI: 10.1124/dmd.106.010801
This article has not been copyedited and formatted. The final version may differ from this version.

TABLE 2. Permeability values of glabridin across isolated perfused rat ileum with mesenteric vein cannulation.

Concentration of glabridin in perfusion solution	$P_{lumen} \times 10^{-4}$ (cm/sec)	$P_{blood} \times 10^{-5}$ (cm/sec)	Ratio of P_{lumen}/ P_{blood}
0.1 μM	6.51 ± 0.72	8.63 ± 0.97[a]	7.54
+ Verapamil (100 μM)	6.64 ± 0.63	21.32 ± 3.12[a,b]	3.11
+ Probenecid (200 μM)	6.57 ± 0.59	9.23 ± 1.14[a,c]	7.12
+ MK-571 (100 μM)	6.72 ± 0.43	9.55 ± 1.03[a]	7.12
+ Celecoxib (100 μM)	6.48 ± 0.59	8.65 ± 1.12[a]	7.49
0.5 μM	8.22 ± 0.91[c]	10.23 ± 1.17[a,c]	8.04
+ Verapamil (100 μM)	8.42 ± 0.63	28.31 ± 3.05[a,b]	2.97
+ Probenecid (200 μM)	8.28 ± 0.51	11.13 ± 1.27[a]	7.44
+ MK-571 (100 μM)	8.40 ± 1.01	10.83 ± 1.37[a]	7.76
+ Celecoxib (100 μM)	8.24 ± 0.61	11.01 ± 1.06[a]	7.48
2.0 μM	11.54 ± 1.31[c]	14.42 ± 1.55[a,c]	8.00
+ Verapamil (100 μM)	12.24 ± 1.41	36.79 ± 4.07[a,b]	3.33
+ Probenecid (200 μM)	11.89 ± 1.41	13.93 ± 1.63[a]	8.54
+ MK-571 (100 μM)	12.22 ± 1.42	16.67 ± 1.82[a]	7.33
+ Celecoxib (100 μM)	12.04 ± 1.61	15.48 ± 1.95[a]	7.78

Data are the mean ± SD. P_{lumen} = permeability calculated based of drug disappearance in intestinal lumen; P_{blood} = permeability calculated based of drug appearance in mesenteric vein.

[a] $P < 0.05$, P_{blood} vs P_{lumen}.

[b] $P < 0.05$, P_{blood} in the presence of an transporter inhibitor vs P_{blood} in the absence of an transporter inhibitor.

[c] $P < 0.05$, P_{blood} at 0.5 or 2.0 μM vs P_{blood} at 0.1 μM.

DMD Fast Forward. Published on January 12, 2007 as DOI: 10.1124/dmd.106.010801
This article has not been copyedited and formatted. The final version may differ from this version.

TABLE 3. The pharmacokinetic parameters (n = 6) of glabridin at 5 mg/kg by gavage with or without combined oral verapamil at 25 or 100 mg/kg.

Parameter	Glabridin (5 mg/kg) alone	Glabridin + Verapamil (25 mg/kg)	Glabridin + Verapamil (100 mg/kg)
$AUC_{0\text{-}24h}$ (ng/ml•h)	97.41 ± 34.58	116.21 ± 36.36[a]	170.52 ±52.28[a,b]
$AUC_{0\text{-}\infty}$ (ng/ml•h)	104.81 ± 35.16	125.22 ± 37.29[a]	183.11 ± 53.62[a,b]
C_{max} (ng/ml)	15.02 ± 4.59	19.01 ± 5.38[a]	25.38 ± 7.62[a,b]
T_{max} (h)	4.15 ± 0.97	2.25 ± 0.52[a]	2.15 ± 0.46[a]
$t_{1/2\beta}$ (h)	3.20 ± 0.93	3.52 ± 0.96[a]	3.76±0.92[a]
F	7.55	9.02	13.19

Data are the mean ±SD. Pharmacokinetic parameters calculated: AUC = area under the plasma concentration-time curve; T_{max} = Time to maximum plasma concentration; $t_{1/2\beta}$ = elimination half-life; C_{max} = maximum plasma concentration; F = oral bioavailability.

[a] $P < 0.05$, control (glabridin alone) vs combination treatment (glabridin + verapamil).

[b] $P < 0.05$, glabridin + verapamil (25 mg/kg) vs glabridin + verapamil (100 mg/kg).

DMD Fast Forward. Published on January 12, 2007 as DOI: 10.1124/dmd.106.010801
This article has not been copyedited and formatted. The final version may differ from this version.

TABLE 4. A comparison of the plasma pharmacokinetic parameters of glabridin at 5 mg/kg by gavage in *mdr1a(-/-)* and the wild-type mice.

Parameter	*mdr1a(-/-)* mice	Wildtype mice
$AUC_{0\text{-}24h}$ (ng/ml•h)	363.32 ± 122.68	76.13 ± 24.51[a]
$AUC_{0\text{-}\infty}$ (ng/ml•h)	389.32 ± 128.12	81.76 ± 26.12[a]
C_{max} (ng/ml)	52.78 ± 14.81	13.79 ± 3.88[a]
T_{max} (h)	2.25 ± 1.26	2.00 ± 0.82
$t_{1/2\beta}$ (h)	3.54 ± 1.14	2.97 ± 0.89[a]

Data are the mean ±SD. Pharmacokinetic parameters calculated: AUC = area under the plasma concentration-time curve; T_{max} = Time to maximum plasma concentration; $t_{1/2\beta}$ = elimination half-life; and C_{max} = maximum plasma concentration.

[a]$P < 0.05$, *mdr1a(-/-)* mice vs wildtype mice.

Figure 1

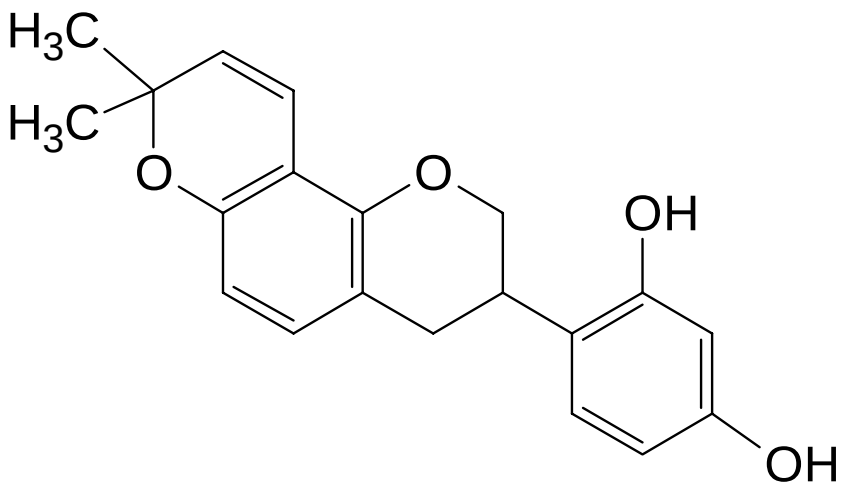

Glabridin

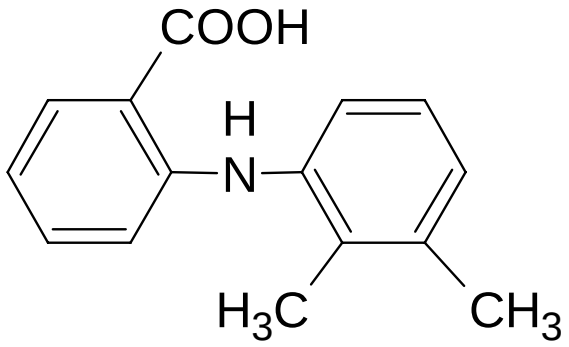

Mefenamic acid

Figure 2

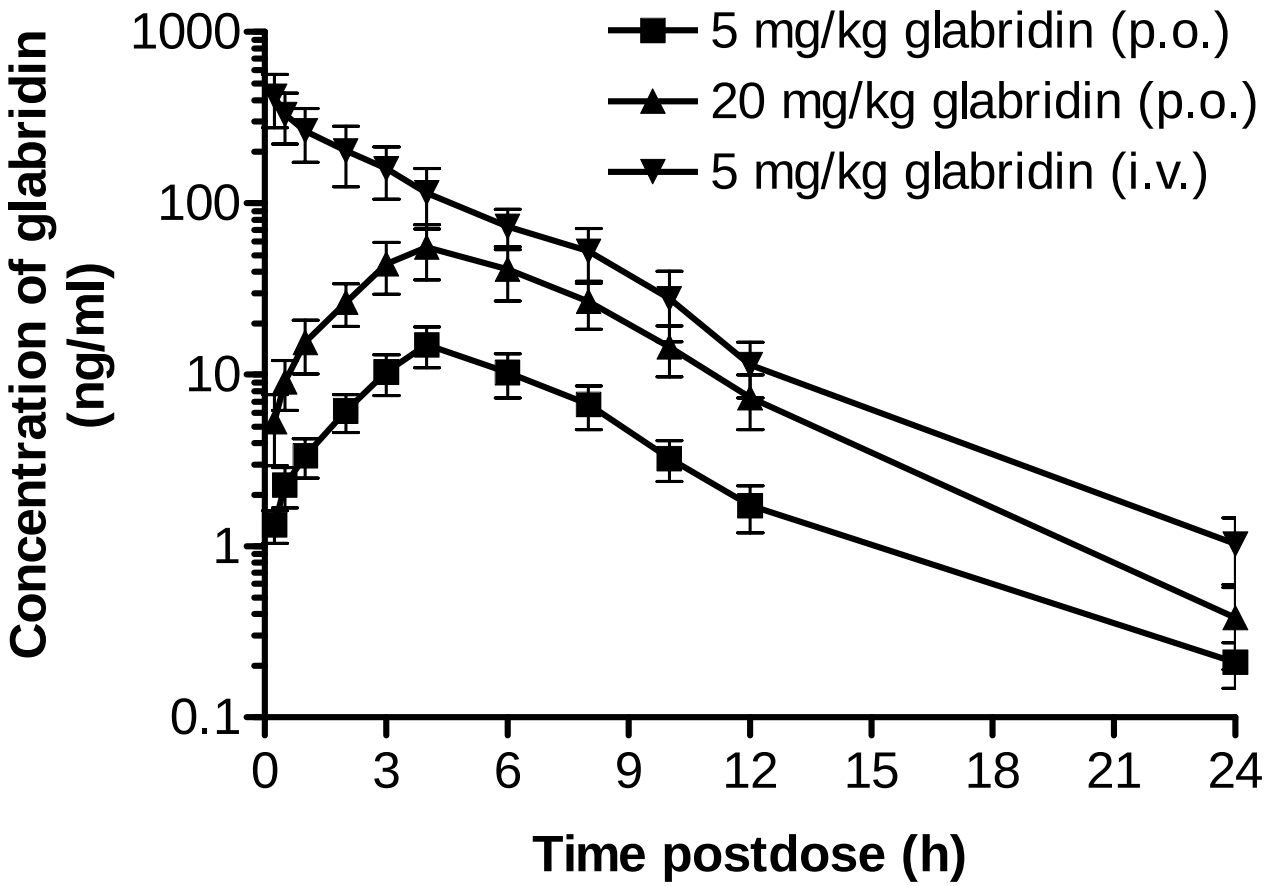

DMD Fast Forward. Published on January 12, 2007 as DOI: 10.1124/dmd.106.010801
This article has not been copyedited and formatted. The final version may differ from this version.

Figure 3

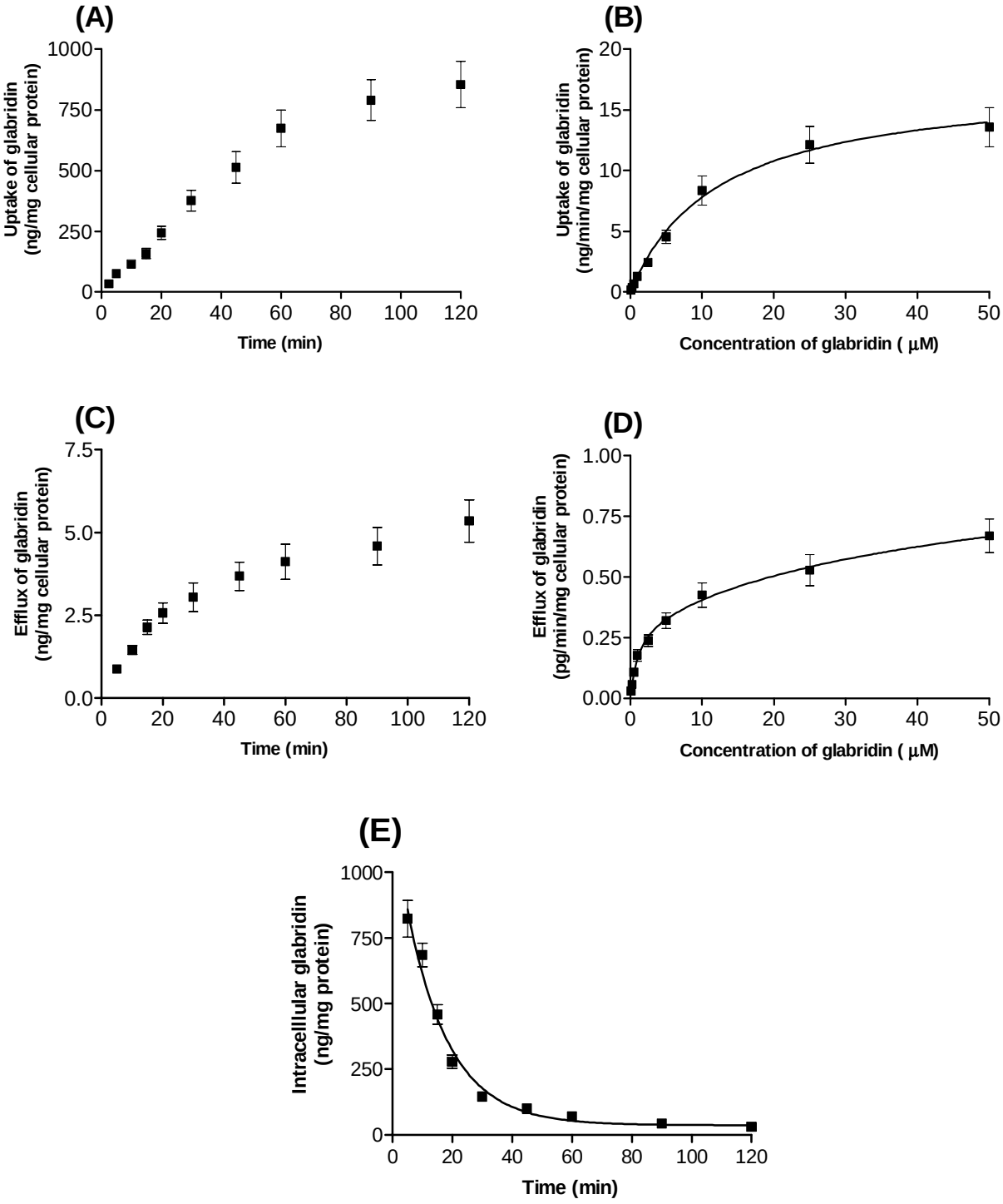

DMD Fast Forward. Published on January 12, 2007 as DOI: 10.1124/dmd.106.010801
This article has not been copyedited and formatted. The final version may differ from this version.

Figure 4

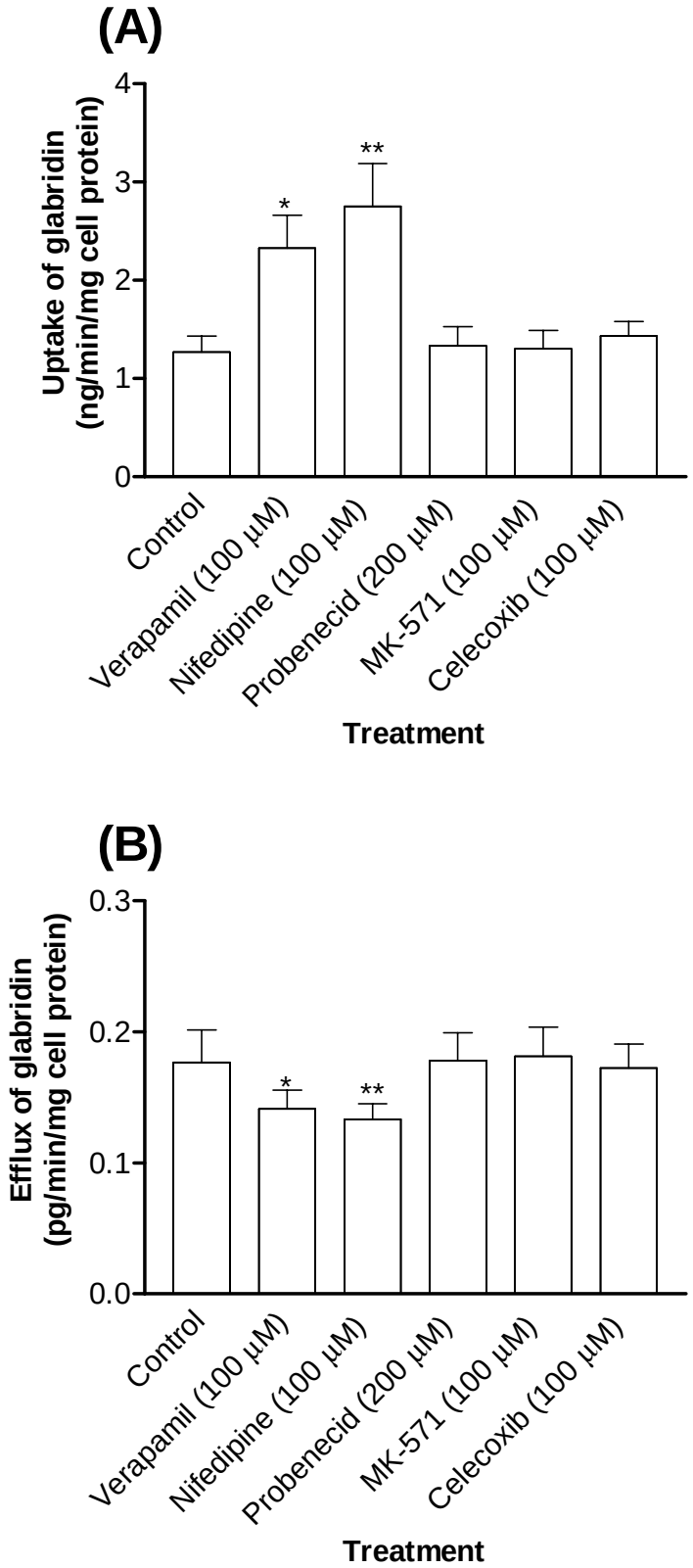

DMD Fast Forward. Published on January 12, 2007 as DOI: 10.1124/dmd.106.010801
This article has not been copyedited and formatted. The final version may differ from this version.

Figure 5

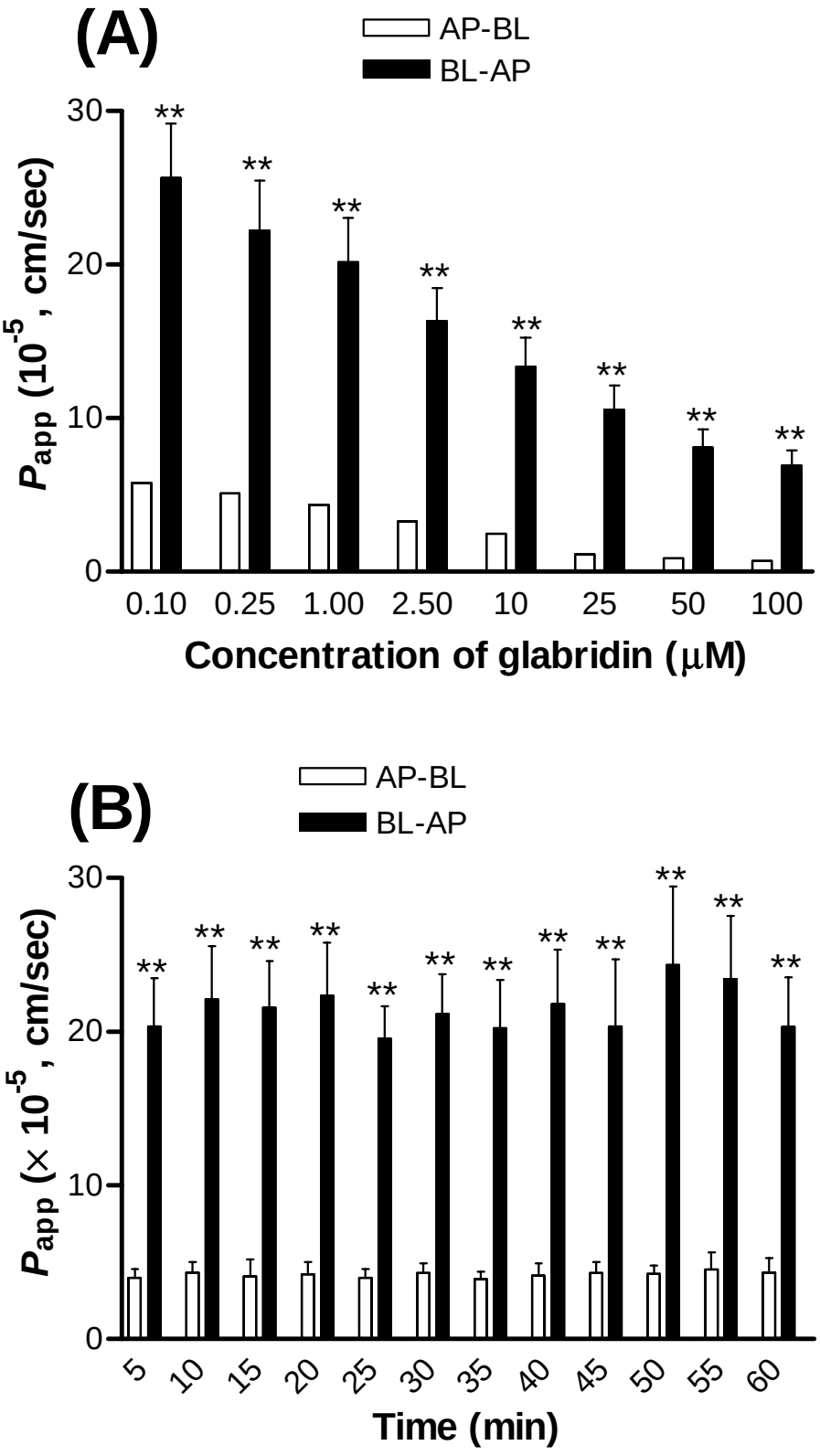

Figure 6

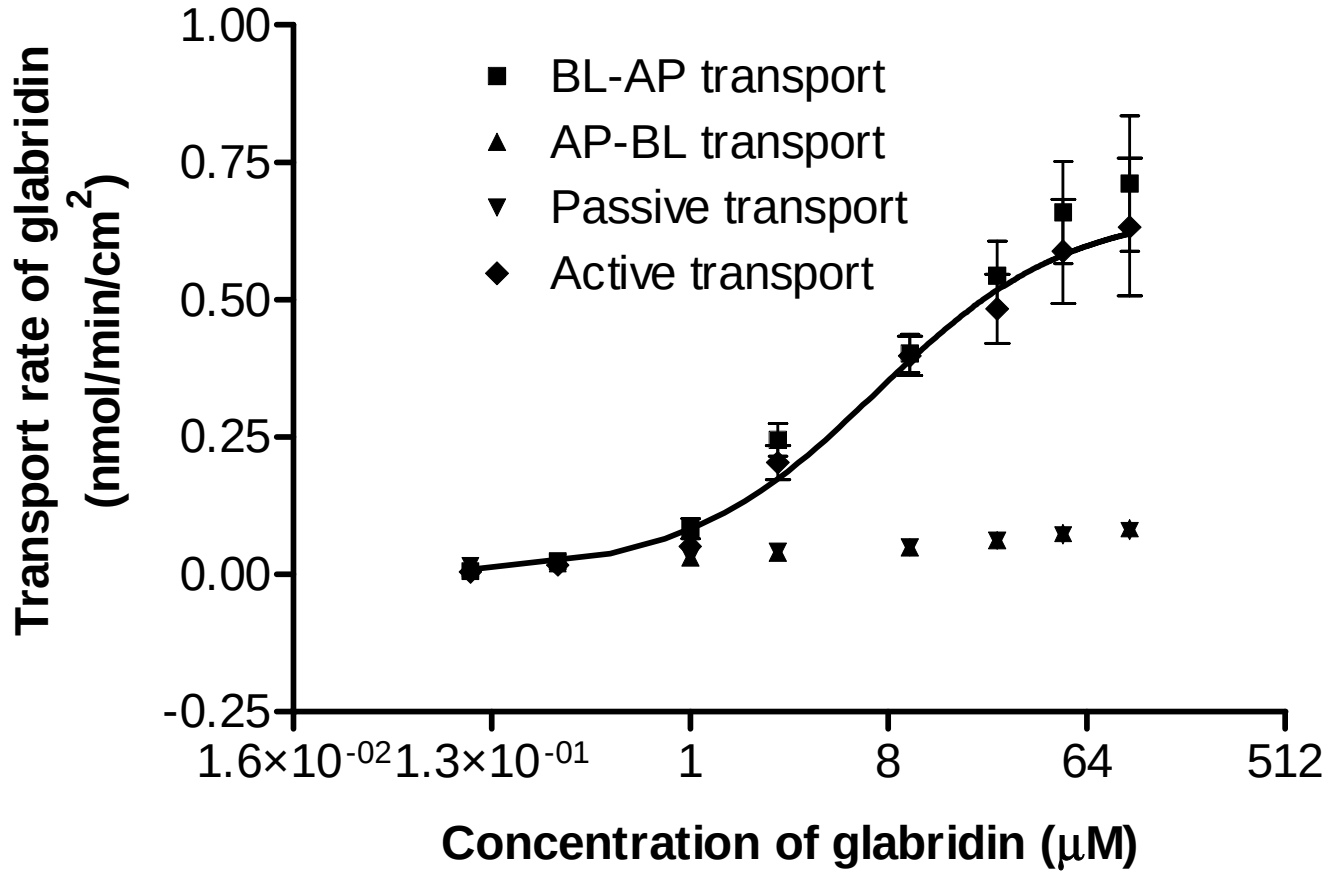

DMD Fast Forward. Published on January 12, 2007 as DOI: 10.1124/dmd.106.010801
This article has not been copyedited and formatted. The final version may differ from this version.

Figure 7

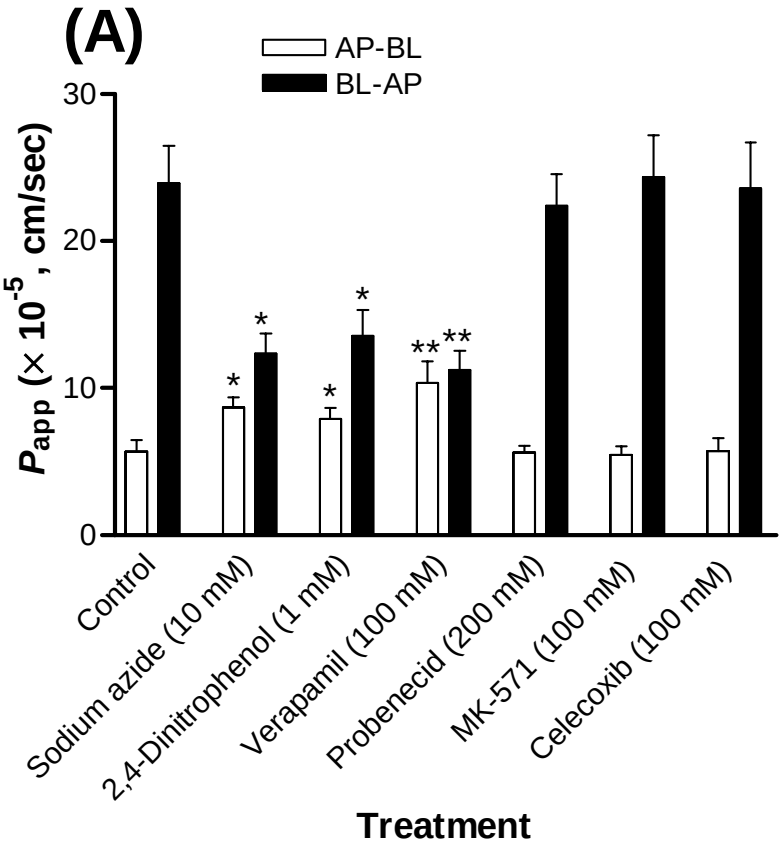

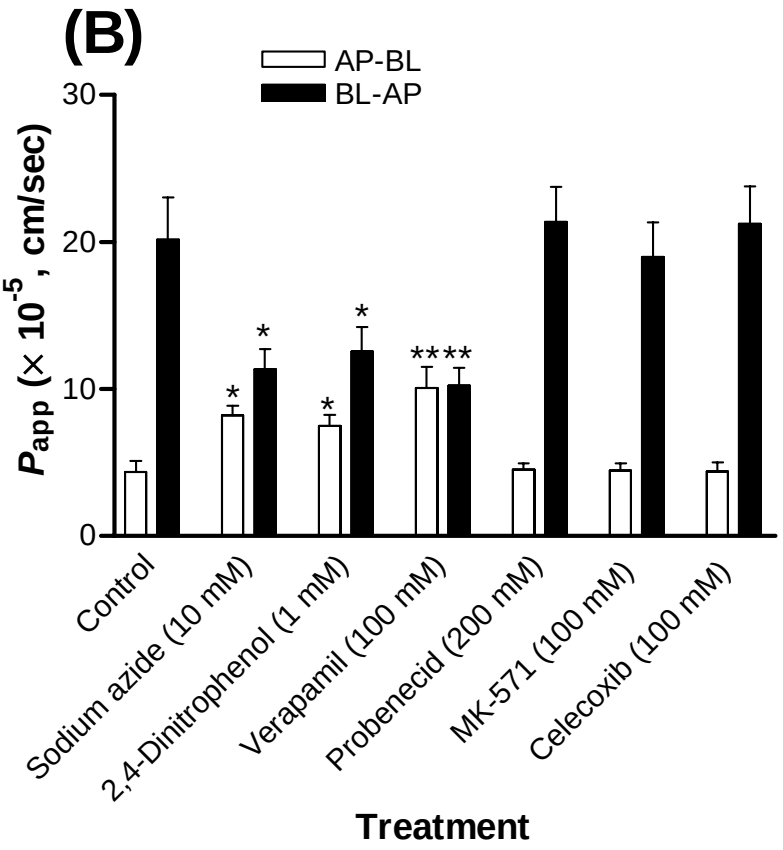

Figure 8

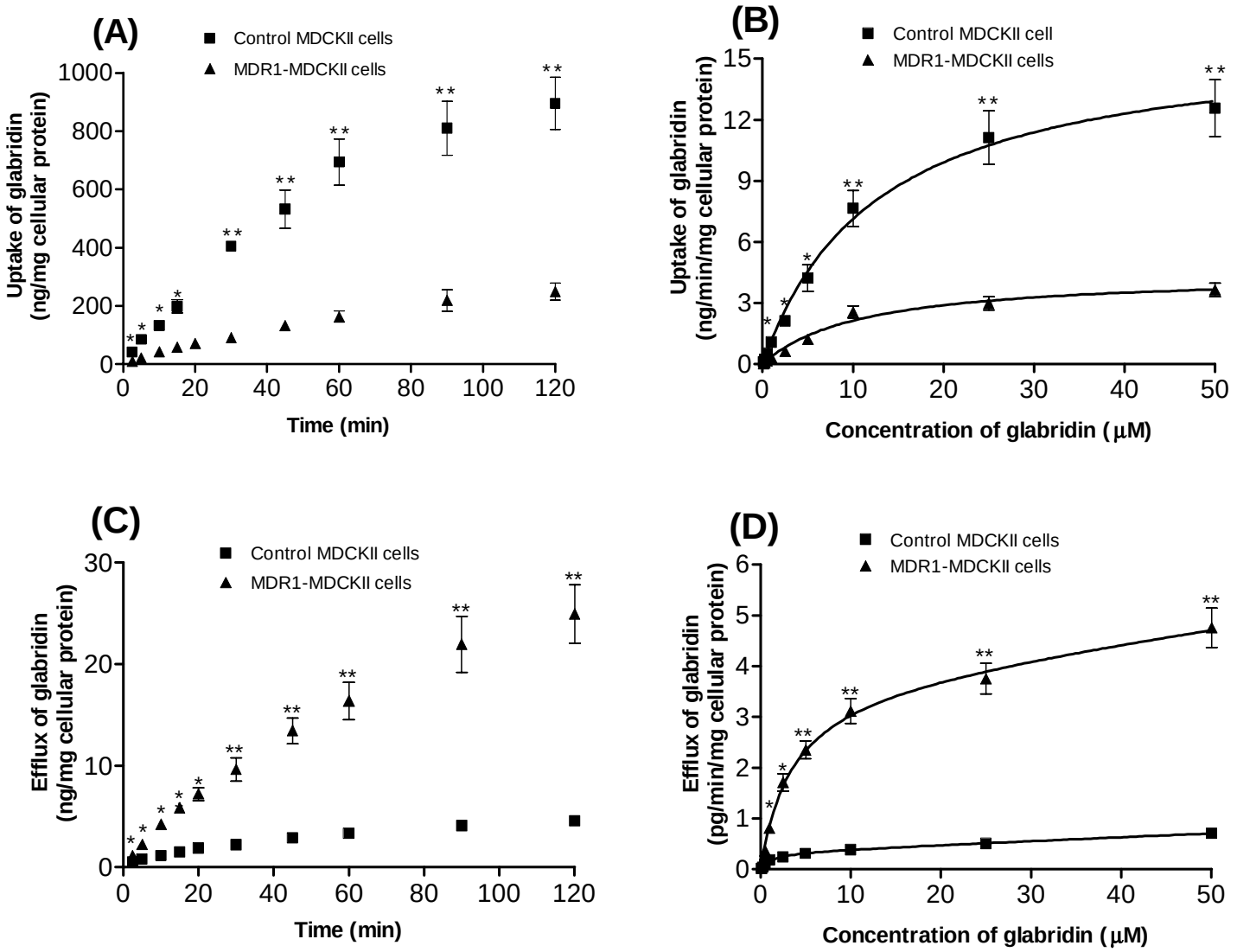

DMD Fast Forward. Published on January 12, 2007 as DOI: 10.1124/dmd.106.010801
This article has not been copyedited and formatted. The final version may differ from this version.

Figure 9

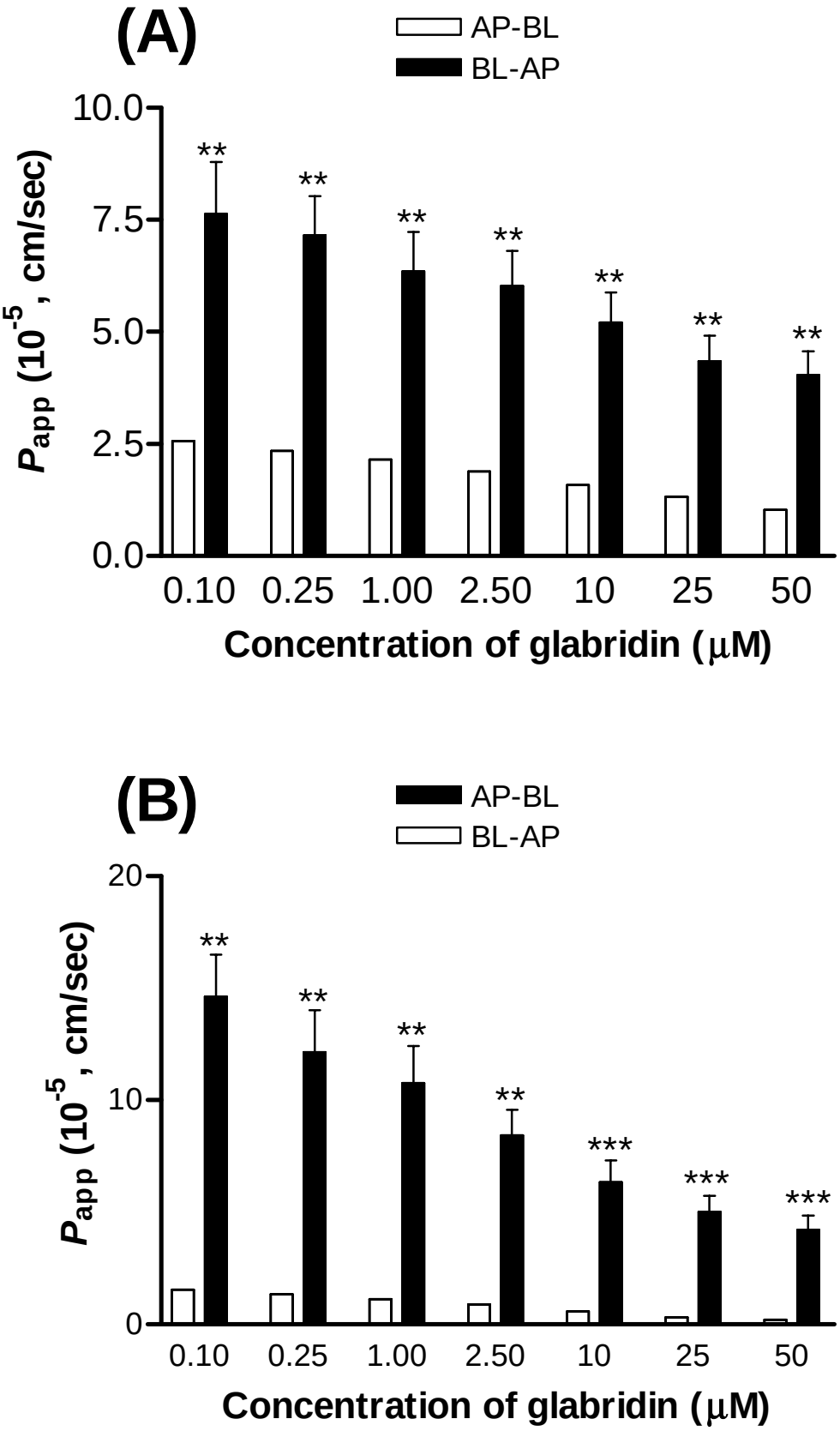

Figure 10

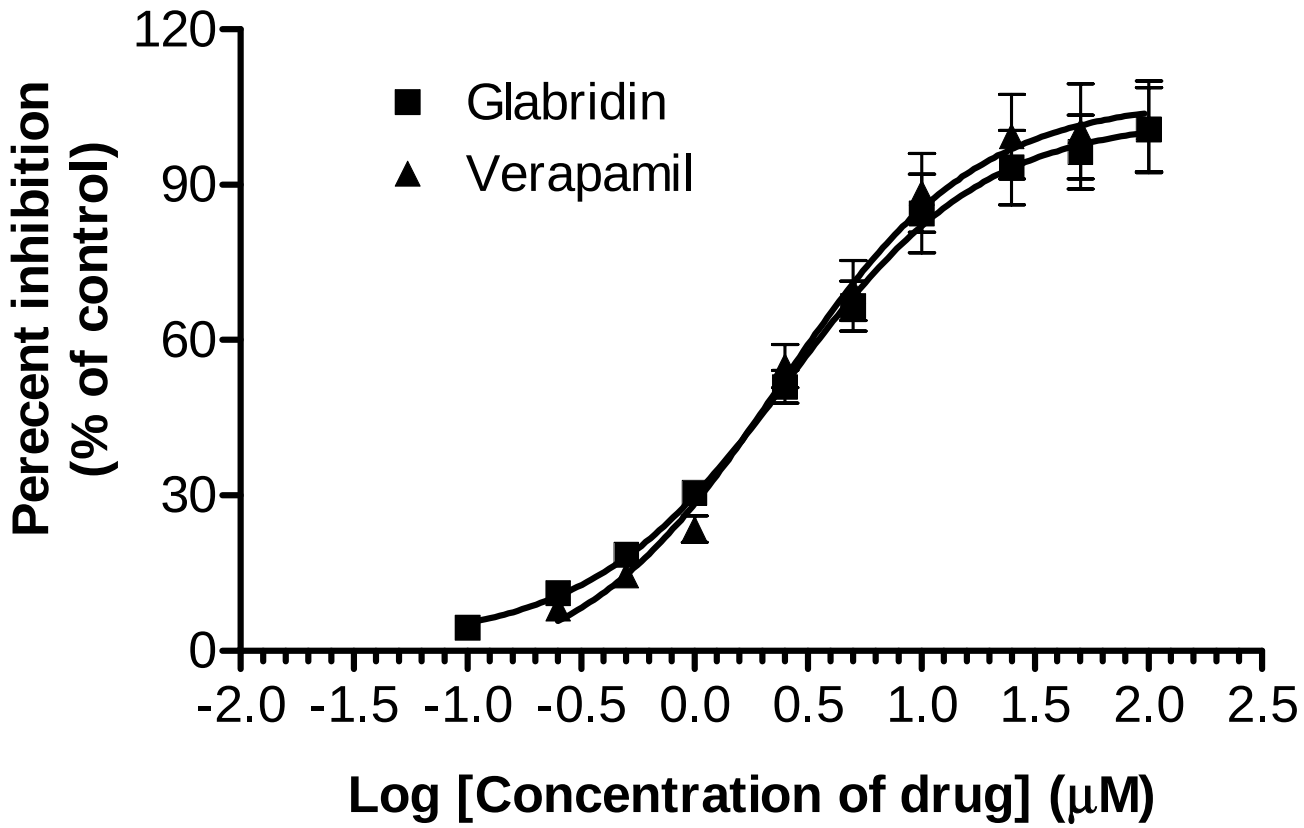

DMD Fast Forward. Published on January 12, 2007 as DOI: 10.1124/dmd.106.010801
This article has not been copyedited and formatted. The final version may differ from this version.

Figure 11

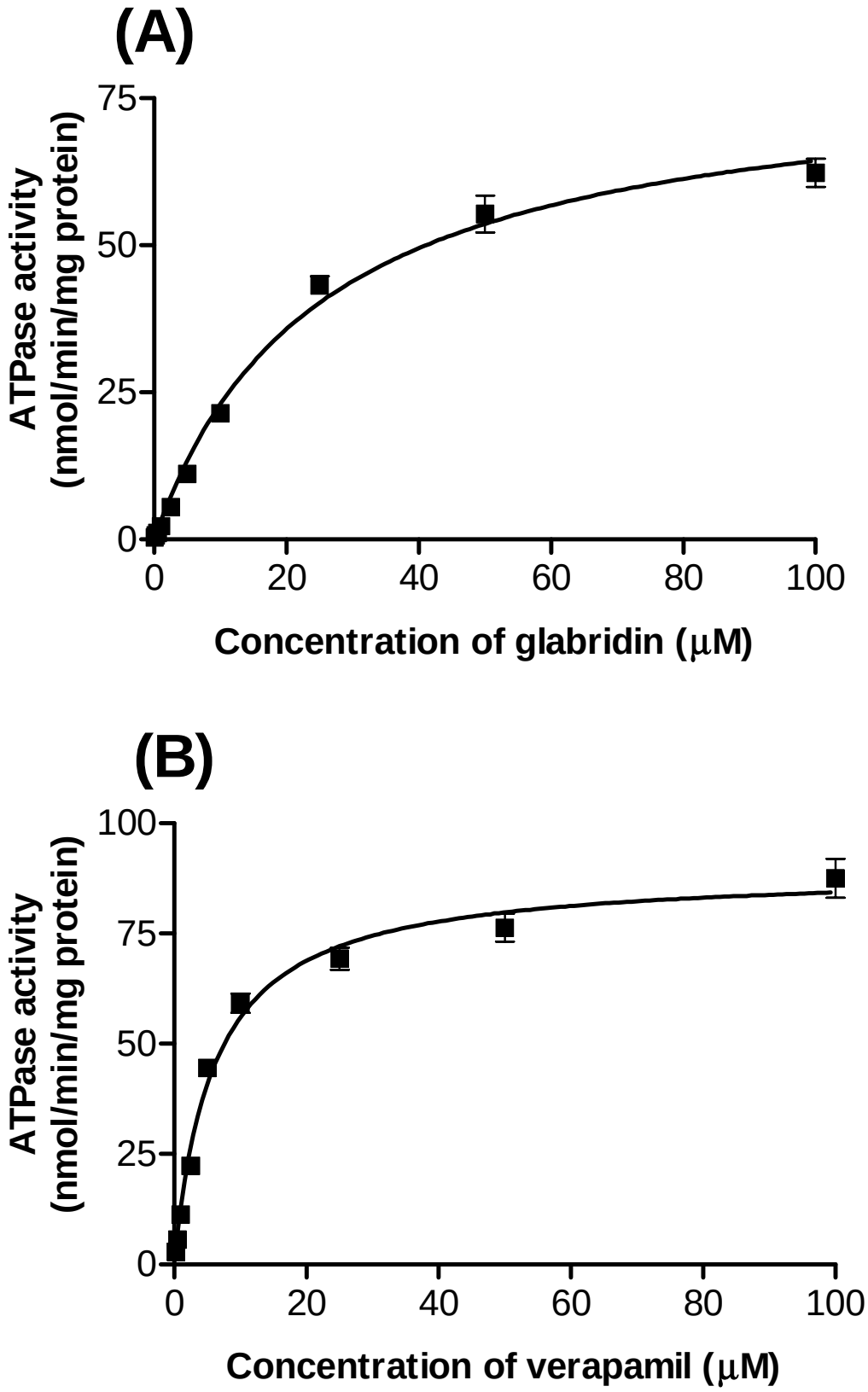

Figure 12

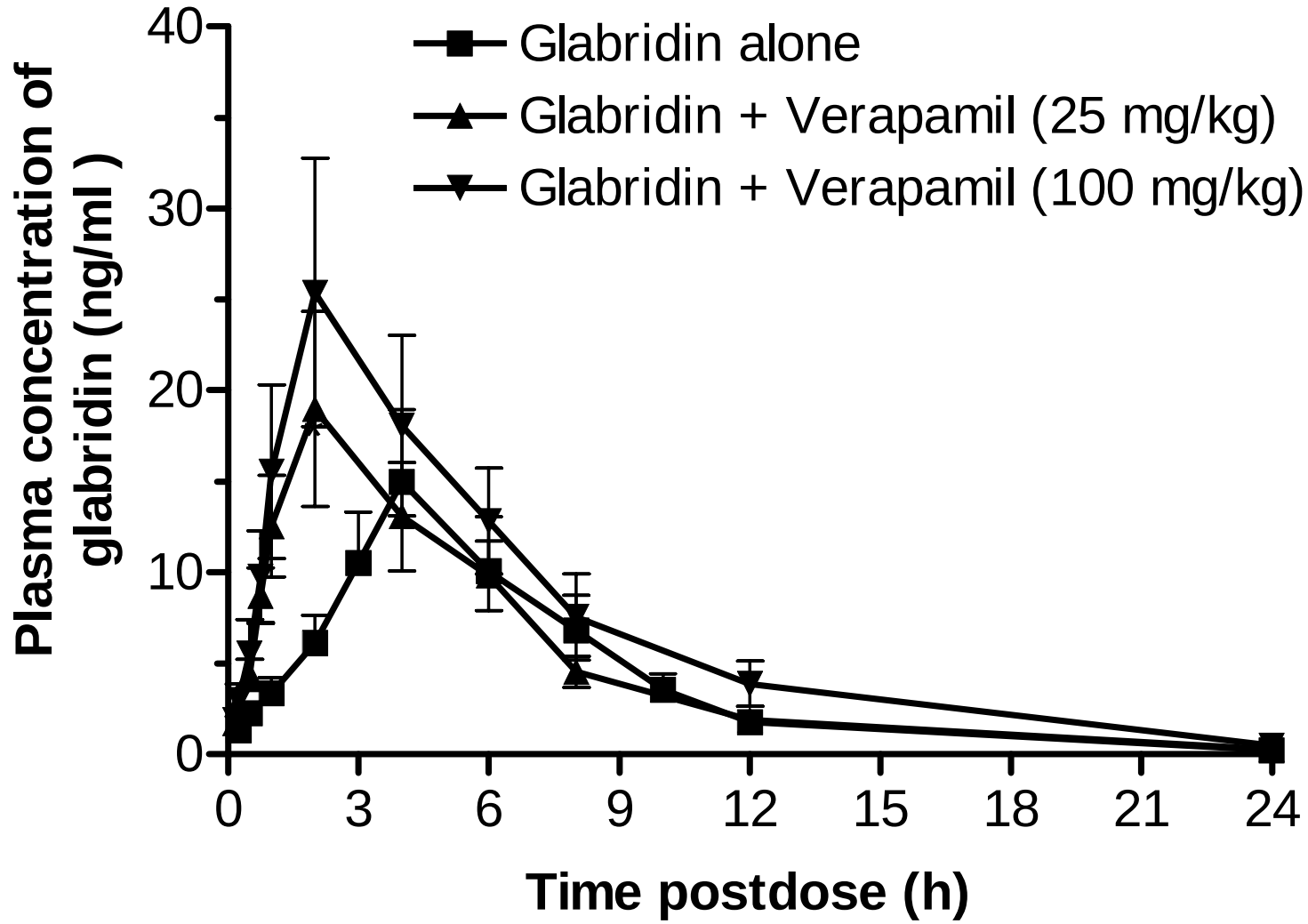

Figure 13